UNIVERSITY OF TURKSH AERNAUTICAL ASSOCIATION
INSTITUTE OF SCIENCE AND TECHNOLOGY

USING THE SECONDARY REFLECTOR FOR IMPROVING HEAT DISTRIBUTION ON THE ABSORBER TUBE

MASTER THESIS

HUSAM MOHAMED ALMAREME

INSTITUTE OF SCIENCE AND TECHNOLOGY
MECHANICAL AND AERONAUTICAL ENGINEERING DEPARTMENT

MASTER THESIS PROGRAM

JANUARY 2019

UNIVERSITY OF TURKSH AERNAUTICAL ASSOCIATION
INSTITUTE OF SCIENCE AND TECHNOLOGY

USING THE SECONDARY REFLECTOR FOR IMPROVING HEAT DISTRIBUTION ON THE ABSORBER TUBE

MASTER THESIS

HUSAM MOHAMED ALMAREME

1506080026

INSTITUTE OF SCIENCE AND TECHNOLOGY
MECHANICAL AND AERONAUTICAL ENGINEERING DEPARTMENT

MASTER THESIS PROGRAM

Thesis Supervisor: Prof. Dr. Cihan KARATAŞ

Husam Mohamed Almareme, having student number 1506080026 and enrolled in the Master Program at the Institute of Science and Technology at the University of Turkish Aeronautical Association, after meeting all of the required conditions contained in the related regulations, has successfully accomplished, in front of the jury, the presentation of the thesis prepared with the title of: "Using The Secondary Reflector For Improving Heat Distribution On The Absorber Tube".

Supervisor : **Prof. Dr. Cihan KARATAŞ**
University of Turkish Aeronautical Association .....

Jury Members : **Asst. Prof. Dr. Reza AGHAZADEH**
University of Turkish Aeronautical Association .....

: **Asst. Prof. Dr. Munir Elfarra**
Yıldırım Beyazit University .....

: **Prof. Dr. Cihan KARATAŞ**
University of Turkish Aeronautical Association .....

Thesis Defense Date: 21.01.2019

UNIVERSITY OF TURKISH AERONAUTICAL ASSOCIATION
INSTITUTE OF SCIENCE AND TECHNOLOGY

I hereby declare that all information in this document has been obtained and presented in accordance with academic rules and ethical conduct. I also declare that, as required by these rules and conduct, I have fully cited and referenced all material and results that are not original to this work.

DATE
21.1.2019
Husam Mohamed Almareame

بِسۡمِ ٱللَّهِ ٱلرَّحۡمَٰنِ ٱلرَّحِيمِ

وَٱلشَّمۡسُ تَجۡرِى لِمُسۡتَقَرّٖ لَّهَاۚ ذَٰلِكَ تَقۡدِيرُ ٱلۡعَزِيزِ ٱلۡعَلِيمِ ﴿٣٨﴾
وَٱلۡقَمَرَ قَدَّرۡنَٰهُ مَنَازِلَ حَتَّىٰ عَادَ كَٱلۡعُرۡجُونِ ٱلۡقَدِيمِ ﴿٣٩﴾ لَا ٱلشَّمۡسُ
يَنۢبَغِى لَهَآ أَن تُدۡرِكَ ٱلۡقَمَرَ وَلَا ٱلَّيۡلُ سَابِقُ ٱلنَّهَارِۚ وَكُلّٞ فِى
فَلَكٖ يَسۡبَحُونَ ﴿٤٠﴾

صدق الله العظيم

سُورَةُ يٰسٓ

ACKNOWLEDGMENT

First, I thank my Allah for helping me to pass all the difficulties that I have got in my work.

I would first like to thank my supervisor Prof. Dr. Cihan Karataş. The door to Prof. Karataş office was always open whenever I ran into a trouble spot or had a question about my research or writing. He consistently allowed this paper to be my own work, but steered me in the right the direction whenever he thought I needed it.

I cannot forget my dear wife (Enas Hassan) who was supporting me in my studies

Last, I thank all people who have supported this research directly or indirectly.

TABLE OF CONTENTS

LIST OF FIGURES

LIST OF TABLES

TABLE OF ABBREVIATIONS

Symbols List

A_i : Cross sectional area of segment i
b : Interaction coefficient
C : Geometric concentration ratio of tubular absorber
Cp : Heat capacity
D_{abi} : Imier diameter of absorber pipe
D_{abo} : Outer diameter of absorber pipe
D_{gi} : Inner diameter of glass envelope
D_{go} : Outer diameter of glass envelope
D_o : Mean Earth-sim distance
E : The equation of time
f : Friction factor
F : The collector efficiency factor
f : The parabola focal length
F_r : Heat removal factor
h : Enthalpy
HTF : Heat transfer fluid
HTF : Heat transfer fluid
I : Extraterrestrial radiation
I_b : Beam radiation
I_{bn} : Beam radiation in direction of rays
I_d : Diffuse radiation
I_o : Solar constant
k : Thermal conductivity
K(0) : Incident angle modifier
L_{loc} : Longitude of the a location
L_{st} : Standard meridian of a local zone time
m : Mass flow rate
n : Day of the year
Nu : Nus se It number
Pr : Prandtl number
PTSC : Parabolic trough solar collector
Q_{gain} : Heat gain
$Q_{heat\ loss}$: Heat loss
Re : Reynolds number
r_r : Mirror Radius
RT : Receiver tube
SR : Secondary reflector
ST : Solar time
T_a : Ambient temperature

T_{abi} : Temperature of inner absorber tube
T_{abo} : Temperature of outer absorber tube
T_{gi} : Temperature of inner glass envelope
T_{go} : Temperature of outer glass envelope
T_{HTF} : Temperature of heat transfer fluid
T_{in} : Temperature at the inlet of PTSC
T_{out} : Temperature at the outlet of PTSC
T_s : Sky temperature
U_L : Heat loss coefficient
V : Velocity
W_a : Parabola aperture

Greek Symbols

λ : W. avelength
ω : Hour angle
Ø : Latitude angle
§ : Solar declination
Θ_Z : Zenith angle
α : Solar altitude
γ_{SUN} : Solar azimuth angle
Ø : Angle of incidence
$Ø_r$: Rim angle
η_o : Optical efficiency
ηth : Thermal efficiency
ρcl : Mirror reflectance
τ : Transmittance
α : Absorptance
$\mathcal{E}$: Emissivity
γ : The intercept factor
ρ : Density
β : Volumetric thermal expansion coefficient
σ : Stefan-Boltaman c onstan

ABSTRACT

USING THE SECONDARY REFLECTOR FOR IMPROVE HEAT DISTRIBUTION ON THE ABSORBER TUBE

Husam MOHAMED ALMAREME
Master, Department of Mechanical Engineering
Thesis Supervisor: Prof. Dr. Cihan Karataş
December 2018

In this thesis, the experimental model is applied to study the performance of parabolic trough solar collector (PTSC) after adding a secondary reflector (SR) on it. In these experimental tests, a main reflector was constructed with dimensions (100 cm - 60 cm). A secondary reflector has been added to the system, both have been made of stainless steel because Its ability to resist rust and weather conditions is high (PTSC and SR). tracking of the sun was by hand movement. Water is used as a liquid to transfer heat within the system because of its rapid heat gain from the absorbent tube wall. The experimental tests have been conducted at the University of Turkish Aeronautical Association in Ankara with climate conditions (31C^{o} - 35C^{o}) during selected days of August. The experiments were achieved in two stages, the first on the parabolic trough solar collector (PTSC) and the second on the parabolic trough solar collector with secondary reflector (PTSC-SR) and were compared in several respects. The performance of PTSC and PTSC-SR is evaluated by using outdoor experimental measurements including the useful heat gain, the thermal efficiency and the heat loss. Note that on the second experimental day the temperature was greater. The results indicate that the greatest temperature of PTSC was 29C at 2:00PM when it exit, while it was for PTSC-SR 28.8C at 2:30 PM. However, most of the hours of the experiment were very close or slight increase for the PTSC. Thermal gain and thermal efficiency were better for the PTSC, however, the thermal distribution was more homogeneous for the secondary reflector PTSC-SR.

Key Words: Secondary, Reflector, Absorber Tube, Parabolic, Reflector, Distribution

ÖZET

EMİCİ TÜP'TE ISI DAĞILIMINI GELİŞTİRMEK İÇİN SEKONDER REFLEKTÖR KULLANMA

Husam MOHAMED ALMAREME
Yüksek lisans, Makine mühendisliği
Tez Danışmanı: Prof. Dr. Cihan Karataş
Aralık 2018

Bu tezde, parabolik oluk tipi güneş kolektörünün (PTSC) üzerinde sekonder reflektör (SR) eklendikten sonra bu güneş kolektörünün nasıl çalıştığını incelemek için deney modeli uygulanmıştır. Bu deney testlerinde temel reflektörler (60cm-100 cm) boyutlarda yapılmıştır. Sekonder bir reflektör sisteme eklenmiş, her iki reflektör toza ve hava koşullarına direnişinin yüksek olması nedeniyle paslanmaz çelikten yapılmıştır. Suyun emici tüp duvarından ısı kazanımı hızlı olduğundan sistem içerisinde ısı transferi için su kullanılmaktadır. Ankara'daki Türk Hava Kurumu Üniversitesinde ağustos ayının belirlenmiş günlerinde (31-35C°) hava koşullarnda deney testleri yapılmıştır. Deneyler iki aşamada yürütülmüştür.Birincisi parabolik oluk tipi kolektörler üzerinde (PTSC) ve ikincisi ise sekonder reflektörlü (PTSC-SR) parabolik oluk tipi kolektörler üzerinde yapılmış ve bir çok yönden karşılaştırılmıştır. PTSC ve PTSC-SR'nin performansı, kullanışlı sıcaklık kazanımı, sıcaklık yeterliliği ve sıcaklık kaybı gibi açık alan deney ölçümleri kullanılarak değerlendirilmiştir. İkinci deney gününde sıcaklık daha fazlaydı. Sonuçlar PTSC'nin en yüksek derecesinin öğleden sonra saat 2:00'de 29 C° olduğunu, PTSC-SR'nin en yüksek derecesinin öğleden sonra saat 2:00'de 28.8C° olduğunu göstermiştir. Deeney saatleri birbirine çok yakın veya PTSC deneyi için çok az daha yüksekti. Isı kazanımı ve ısı etkinliği PTSC'de daha iyiydi,ancak ısı dağılımı sekonder reflektör PTSC-SR'de daha homojendi.

Anahtar Kelimeler: İkincil, Reflektör, Soğurma Borusu, Parabolik, Reflektör, Dağıtım

CHAPTER ONE

INTRODUCTION AND BRIEF HISTORY

1.1 Introduction

In recent years, the focus has been largely on the uses of solar energy, its ability and high efficiency in transforming solar energy to electric energy, mechanical energy and thermal energy. The impact of renewable energy and specially the solar energy on the environment is one of the main reasons for its development. Solar energy researches have seen great progress in recent years. Without a doubt, moderate weather, which tends to high temperatures, will greatly help in the continued use and development of solar energy. Turkey is one of the countries that has mild weather, although winter is long but generally has high solar radiation and high temperatures from May to November Where solar radiation reaches 1700 kw/h. In this study, it has been compared the parabolic trough solar collector and the parabolic trough solar collector with secondary reflector developed to improve the efficiency and effectiveness of the absorbent tube mainly.

1.2 Brief About The Energies

In recent years, energy consumption has increased significantly as pollution has increased. According to a 2012 study, the utilization of alternative energy is expected to increase by more than a third in 2035 [1]. Fossil fuels remains as a major and the main source of energy supply in the world. As per to the publications of international energy studies, large portion of energy nears to 84.7% is derived from fuels of fossil, which has a considerable impact on the environment. The Energy and Climate Change Agency (DECC) predicted that fossil fuel prices could reach $ 135 by 2030.3 This high cost is affecting poor countries that are not able to spend a lot of money to meet the costs of fossil fuels. The energy needs of the population on the

other hand, fossil fuel carbon dioxide products have significant environmental effects, including rising global temperatures. According to the International Energy Agency (IAE), in 2010 the emissions od CO2 gas from fossil fuels approaches to 30.326 million tonnes, whereas it was around 1973 is just 15.637 million tones [3]. The aforementioned environmental issues and economical problems are pushed the consumers in the world to sustainable energy sources to provide environmentally green energy, reducing the need for fossil energy sources, as well as its impacts on the environment. environment and the economy.

Solar energy is considered as one of feasible sources of green energy in the world, which is one of the techniques usefully applied in this field, the parabolic trough solar collector (PTSC) will be recognized. identify one of the flaws in this system and try to find a solution to this problem.

1.3 Parabolic Trough Technology Developments

An incredible level and amount of developments have been made on the solar reflector since its first manufacture in 1870 by the Swedish engineer John Ericsson with an opening of 3.25 m^2 for this device. Its goal was to generate steam to run a 373.5W engine. Retrospectively, over the years, same alike first proposed system, the Ericsson is proposed a new seven systems. The first reflector was built by Ericsson in 1883; it was relatively large compared to previous devices. The dimensions of the same is about 4.88 meters in width and 3.35 meters in length, the parabolic diameter is set to be 15.88 cm [4]. Adolf Remshardt and Wilhelm Meier in the 1907in Germany have rewarded a patent for their contribution in the parabolic trough sensor studies, the main agenda of their system that been proposed is to produce the steam using the solar energy [5]. Frank Shuman, an engineer from the United States, has conducted many experiments on different types of solar collectors that pump irrigation water in Tacony, Pennsylvania. It was from 1906 to 1911. After gaining experience in this area, he established a large water pumping system in 1912 in a small village near Cairo, Egypt, with the station shown in Figure 1.1. An English consultant, named; Charles Vernon, who oversees this system with Frank Shuman, advised that the pipe be covered with a glass plate along the (PTSC), consisting of five rows of (PTSC) with dimensions of width of 4.1 meter and length of 62.17 meter and 1250 square meter is the area of mounting surface which is occupied a land of

area closed to 4047 square meter [4, 6] the established system is generating a water in capacity of 27,000 L/min [5].

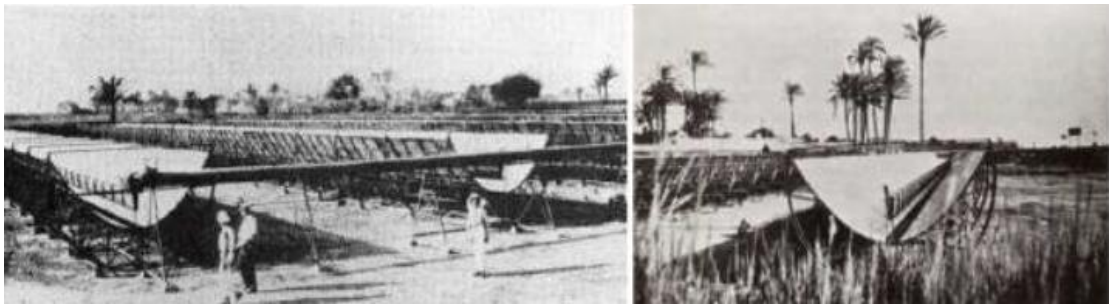

Figure 1.1: Irrigation pump plant in Egypt. Adopted from [5].

C.G. The steam engine and the PTSC were utilized by Abbot to turn solar energy into mechanical power during of 1936. In order to reduce heat loss, he utilized along the PTSC a double-wall vacuum-clad insulated tube planted. The paradigm was established to generate a steam with saturation 374 post putting the PTSC on the sun target for around five minutes of time [4, 6].

The advancement of the level of technology (PTSC) ceased 60 years later, and later in the mid-1970s. After rising oil prices, in the mid-1970s, Sandia National Laboratories and Honeywell International Inc. have made a couple of collectors. United States of America during the 1970 is intended to obtain the same system to perform on temperatures lesser than 250. Afterward, in 1976, three PTSCs were establish and tested at Sandia for a length of 3.66 m, a width of 2.13 m and an absorber coated with black chrome and covered with a 4 cm glass envelope [7].

LUZ International, is a company established in united states of America during the 1979, they aimed to design solar heat and thermal applications in cost efficient means, heat sensors are designed by the same. Three types of new parabolic sensors are designed by LUZ company which are called as LS series such 1, 2 and 3 of LS sensor as demonstrated in the figure 1.2. in Solar Power Generation System (SEGS), the mentioned system was inaugurated. In the preliminary types such as, LS-1 and LS-2 the assemblies are aligned identically. The sensors are designed to perform the thermal operation in solar system with three variances such as LS1 through LS3, all are tested under different environmental conditioned and proven a noticeable performance.

Figure 1.2: LS-collector 3.

During the period of the 1980s, most American companies already manufactured and sold parabolic bucket sensors, for example:

a. Acurex 3001 and 3011 are both models which are fabricated by Acurex Solar Corp.
b. Model 360 and model IV are fabricated by Suntec Systems Corp and Excel Corp.
c. T800 model and T700 model are fabricated by Solar Kinetics Corp.
d. The IND-300 model built with Solel solar energy.
e. And notably:
f. The parabolic gutter sensor model IV built by Suntec Systems Inc.

By the year 1988, the advancement and the establishment of a new generation of PTSC was the goal of a group of European research companies and laboratories created for this purpose. The new model ET 100 initial reading was conducted using post considering a multiple collectors' models. The model contained 8 modules with an area of 545 m^2. After that, the second type was developed, also it named ET-150. This type included a number of modules of 12 with an area of 820 m2 [8]. In the year 2003, built the third version of the European collector, SKAL-ET is the name that he had allotted. The same included a multiple module of 12 with an effective opening area of 4360 m2. It had been built at the SEGS-V plant in California, USA since that time. [4] In the year 1936, C.G. The steam engine and the PTSC were utilized by Abbot to turn solar energy into mechanical power. The clad vacuum of double wall insulated tubes is used to eliminate the thermal losses along the PTSC. The prototype is expected to generate a steam of 374 post five minutes od time exposure into sunny area [4, 6].

The advancement of the level of technology (PTSC) ceased 60 years later, and later in the mid-1970s. After rising oil prices, in the mid-1970s, Sandia National Laboratories and Honeywell International Inc. have made a couple of collectors. United States of America during the 1970 is intended to obtain the same system to perform on temperatures lesser than 250. Later, in 1976, three PTSCs were structured and tested at Sandia for a length of 3.66 m, a width of 2.13 m and an absorber coated with black chrome and covered with a 4 cm glass envelope [7].

LUZ International Inc, is a company established in united states of America during the 1979, they aimed to design solar heat and thermal applications in cost efficient means, heat sensors are designed by the same. Three types of new parabolic sensors are designed by LUZ company which are called as LS series such 1, 2 and 3 of LS sensor as demonstrated in the figure 1.2. in Solar Power Generation System (SEGS), the mentioned system was inaugurated. In the preliminary types such as, LS-1 and LS-2 the assemblies are aligned identically. The sensors are designed to perform the thermal operation in solar system with three variances such as LS1 through LS3, all are tested under different environmental conditioned and proven a noticeable performance.

Spanish company SENER have created a device known as SENERTROUGH-I as new PTSC prototype. The device was holding the same properties of LS2 and Ls3 manifolds where the LS3 is preserving the similar size and LS2 is preserving the similar structural supports. Installation of the loop in 600 meters in collector that called SENERTROUGH-I in the Andasol was focusing the solar Spain installation was taking place. Currently, PTSC is having a several kinds, some kinds are under experiments and others are available in the markets [5].

a. For establishing and developed design named as Solel-6, Solel Solar System is paying efforts for the same. This design is seemed like LS3 with structural variance.
b. New DSG collector is fabricated by German company called as The Solarlite with intension to produce a steam with 400 ° C temperature. The technology of the same is deployed in double pilots' aircrafts.
c. new collector known as Sky Trough is fabricated by company called as The Sky Fuel. The LS3 is holding the similar dimensions of this prototype with reflective surface difference, this collector is inexpensive and tiny in size

fabricated by Sopogy Micro CSP in united states of America. The length of the same was about 3.66 meter and 1.52 meters of width.

1.4 Heat Transfer Fluid for PTSC

The transfer of fluids by heat transports the heat from the RT into the heat storage tanks of solar heating (and cooling) systems. The most commonly used fluids are water, hydrocarbons, glycol, and air. When selecting a transfer fluid, the following criteria must be taken into account: expansion coefficient, viscosity, heat capacity, freezing point, and boiling point. Each type of fluid has a recommended operating temperature range and its effectiveness decreases as the temperature of the liquid increases. Thus, liquids that can operate at low temperatures will improve the performance of the absorption tube of each type. The fluid has advantages. For example, liquids such as salts may be used as thermal storage devices, but they may also require additional heating during sunlight hours to prevent rigidity of pipes and equipment. Usage can also be affected by costs and availability. As the efficiency of the power cycle increases as the temperature of the working fluid increases, a comprehensive study must be included on both sides of the solar energy cycle. Here are some of the most commonly used heat transfer fluids and their properties.

a. The air does not freeze and boil and is non-corrosive. However, it has a very low heat capacity and tends to leak from collectors, ducts, and dampers. ·
b. While water is cheap and has no toxicity. It is characterized by a high specific heat and a very low viscosity, which facilitates its pumping. Unfortunately, the water has a relatively low boiling point and a high freezing point. If a neutral pH (acidity-alkalinity cannot be maintained, the water can become corrosive. ·
c. And then the hydrocarbon oils have a high viscosity and a lower specific heat than water. They need more energy to pump. These oils are relatively inexpensive and have a low freezing point.
d. While the refrigerants/fluids with phase change, they are commonly used as heat transfer fluid in refrigerators, air conditioners and heat pumps. They usually have a low boiling point and a high heat capacity. The heat absorption occurs when the refrigerant boils (gas-liquid phase) in the solar collector.

And on the other hand, chlorofluorocarbon (CFC) refrigerants, like; Freon, was the major fluids that were utilized by the refrigerators, the air conditioners and as

well as the heat pumps manufacturers because they were non-flammable, low-toxicity, stable and non-freeze [10,11].

1.5 Applications of PTSC

PTSC is available with large variance and hence large population of those devices are found in many applications in industrials and technologies. Listed-out face below justifies and indicates the most relevant and valuable applications.

1.5.1 Solar Power Generation

Solar energy has been applied on a large scale. The integration ofthermal solar power plants and PTSC and can be yielded in couple of possible means:

The first mean is by using DSG technology when the steam turbine runs on steam generated directly from the PTSC.

Secondly, with same range of solar, the fluid of heat exchanger is used to produce the required steam under a known temperature to operate a turbine such as steam turbines.

The whole verities of steam turbines can be run by PTSC in the both cases above involver the overhead rankine and reproduced rankine. The cyle rankine, the warming rankine can be used also for steam production from an organic material where not only water can be used for this kind of operations.

1.5.2 Solar Refrigeration

A technical sample of solar refrigeration is the absorption units powered by PTSC. A thermal absorption refrigeration scheme is shown in Figure (1.3). the system is involving a several components that form the operations of the same, the same can be mentioned as the pumps, generator, absorber, the evaporator, the condenser, the heat exchanger, and the regulators [14]. The PTSCs in the generator applies the refrigerant with heat, along the refrigerant steam exiting the generator flowing to the condenser where rejecting the heat. Then, in order to reduce the pressure, the liquid passes through an expander. The conversion of the liquid to steam of evaporator has took place, evaporator charge of the heat being applied for refrigerants operation. A weak solution can be converted into a strong solution when

the refrigerant vapor is absorbed by the weak fluid. heat rejection is there in the entity of absorber because of to the passage of vapor refrigerant in the liquid steam. By using a pump liquid, the pressure of liquid is increased at the condenser pressure. The solution is strongly preheated in exchanger heat by employing a low and solution hot flow from the generator. It is passed then in to the generator and is warmed till high steam temperature by a solar array field. At the meanwhile, through the heat exchanger and the regulator, the weak solution passes [15].

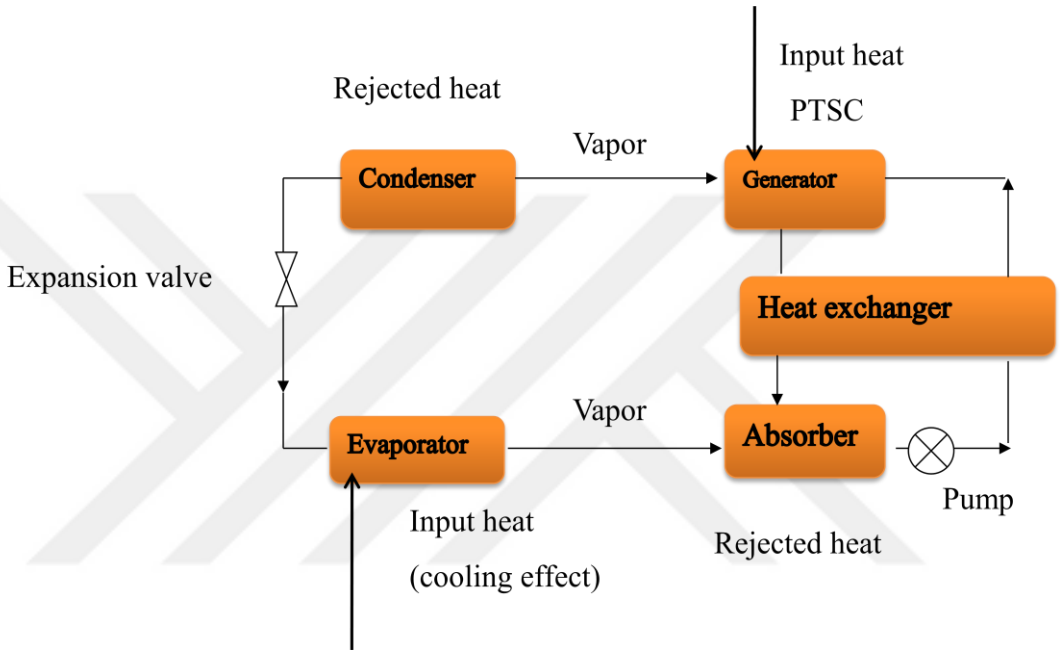

Figure 1.3: Basic principle of the absorption air conditioning process [12].

1.5.3 The Desalination of Solar

Seawater desalination can be achieved with parabolic technology because it is available in several regions of the earth. There will be a couple of groups of water desalination.

a. The system directly collecting the water

b. The system that is collecting the water indirectly

The initial group is directly using PTSC to desalt water salt. The salt water separation and fresh water are obtained by pumping salt water into the tanks; when it flows, it separates. The other group is demanding couple of subsystems; one for desalination and the rest id used for energy collection represented by PTSC. In the PTSCs, a heat transfer fluid is rotated which supplies the required heat to a steam

boiler while the pumping of the salt water is carried out in a steam boiler, fresh water is produced by condensation (16). Other substitutions of the same nature are found too for parabolic gutter sensors, involving the heat treatment in the industrial applications and space heating with hot water, pumping irrigation water ad cooking, solar chemistry and solar cookers. Applications from the same kinds are found inerasably.

1.6 Solar Energy in Turkey

At 2023, the ambitious vision of Turkey envisages particularly interesting goals sustainable for the part of the sectors in energy. The goals are involved an agenda for a minimum of 5000 MW of solar power plants.

The main objective of Turkey the sustainable share is planned to be increased in the sector of energy resources needed to produce electricity by at least 30% by 2023.

About 246,356 GWh was the Electricity consumption and renewable energy sources are responsible to generate about 28% of this consumption Group's is 68,980 GWh approximate contribution, made up of 86% (59,420 GWh), of resources from water,11% (7,557 GWh) of resources winds and 2% (1,363 GWh) and of resources in geothermal biomass (1,171 GWh) [12].

Turkey seems to be very lucky the reason being that; it has a very high level and a high potential in solar energy because of its geographical location. Figure 1.3 below shows the good geographical location of Turkey.

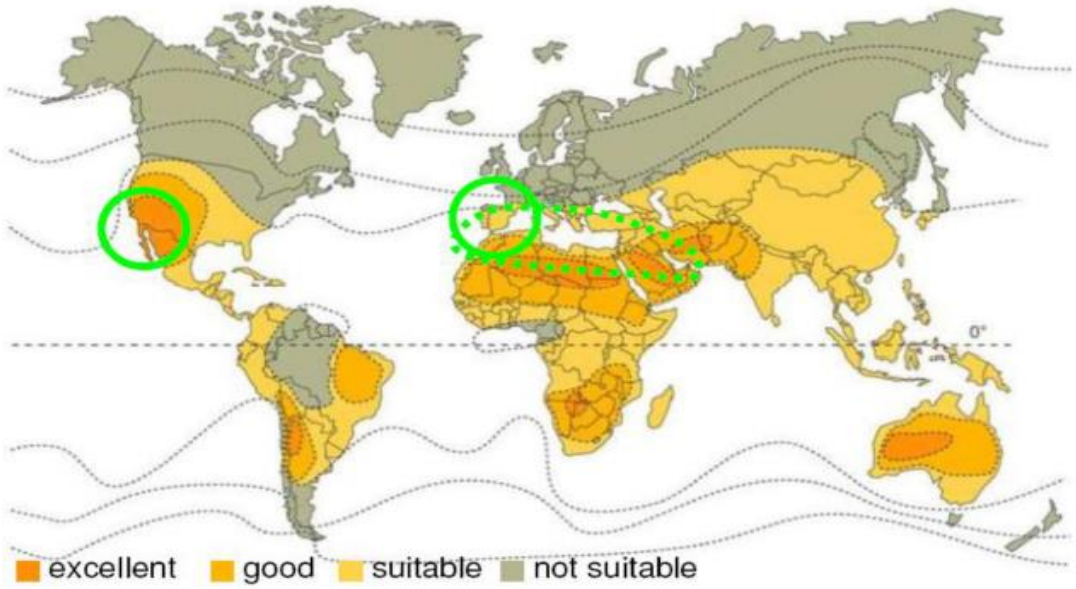

Figure 1.4: The geographical location of Turkey. Adopted from [12].

The distribution of global temperatures is shown in Figure 1.4 below. In accordance with the Turkish Solar Energy (SEM) map where the Renewable Energy Directorate is adopted this map, the total insulation has been determined by this map the time of single year is 2,737 of hours (a whole of 7.5 hours). per single day), and the entire solar derived energy is 1,527 kWh / m^2 per one year (whole of 4,2 kWh / m^2 per one day). In the figure below where you may see the mean value of global solar global radiation in the country of Turkey: 1,500 kWh / m²-year [12].

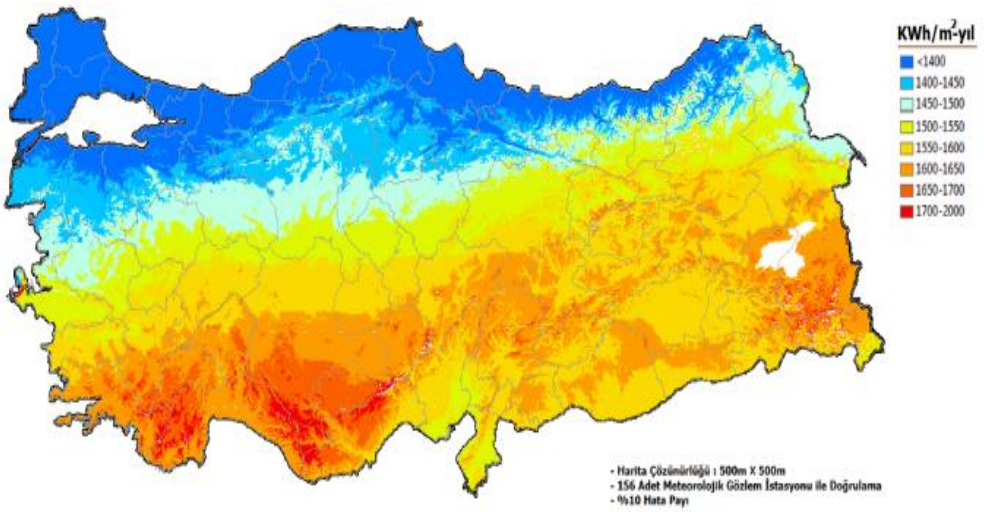

Figure 1.5: Average Global Solar Radiation of Turkey. Adopted from [12].

In 2012, the total area of solar collectors established in Turkey was very near to the 18,640,000 m^2. Calculations showed that the year wise generation of total solar sensors was 1,164,000 m^2, when that of technological vacuum tubed sensors were 57,600 m^2. It is termed as 50 percent of plenum sensors and whole vacuum tubed sensors produced are deployed in the states. The production of thermal energy has been achieved through the use of solar collectors. Calculations showed that thermal energy use was 500,000 PET in homes and 268,000 PET in an industry [12].

1.7 Objectives of the Study

In this type of system there is a major problem, namely, that the absorber tube in the system is exposed to warp during the exposure to high temperatures on the long periods, so the aim of this study is:

a. Determine the size of the secondary reflector, in which it can reverse the maximum amount of solar radiation on the top surface of the absorber tube.

b. Trying reduce the temperature at the bottom of the absorber tube so that we maintain high efficiency for (PTSC).
c. distribute heat regularly on the entire diameter of the absorber tube for two reasons:
    1. Do not warp the absorber tube in the side that exposed to high temperature.
    2. Increase the water temperature because it will gain additional heat from the secondary inverter at the top of the absorber tube.
d. Comparison this model with the conventional model and find the difference between them.

1.8 Organization of The Study

This thesis consists of five chapters which are briefly introduced in the following:

a. Chapter One gives a background about the technology of parabolic trough, also including the historical development of the technology and its applications, turkey interest in solar energy and distribution of solar radiation in Turkey.
b. Chapter Two displays the solar radiation falling on the earth's surface, including solar angles, extraterrestrial radiation, and terrestrial radiation. A model has been developed to evaluate the amount of solar radiation that reaches the earth depending on several factors. In this section, all the equations used in this study are thermal gain, thermal loss, thermal efficiency, this chapter discusses the previous studies that have been achieved regarding the improve the performance of the absorbent tube.
c. Chapter three presents an experimental model of the PTSC-SR in detail. Explain the components of the system and how to install some parts.
d. Chapter four presents the results of testing PTSC and PTSC-SR and comparative between them, also, analysis of efficiency, heat gain and thermal loss.
e. Chapter six presents a conclusion of the experimental study with the recommendations that may be followed for future studies.

CHAPTER TWO

SOLAR EQUATIONS

2.1 Fundamentals of Solar Radiation / Solar Geometry

Through-out the day to day tracking of the sun (24 hours a day), all through-out the year, there has been very peculiar geometric relationships of the position of the collector in regard to the time which was needed to be recognized.

2.1.1 Sun Earth Geometrical Relationship

It is important for us to note that; the Earth rotates around the sun every 365.25 days in an elliptical orbit called the ecliptic plane and performs a full rotation around its axis every 24 hours. The distance between the earth and the sun is the smallest of 21 December (perihelion of 1.47 × 1011 m), while the maximum distance is 21 June (aphelion of 1.52 × 1011 m). The angle of rotation of the Earth's axis at an angle of 23.45 ° to its orbit plane is shown in Figure (2.1). This tilt (inclination) remains fixed and is as a result of the seasons all year long [13].

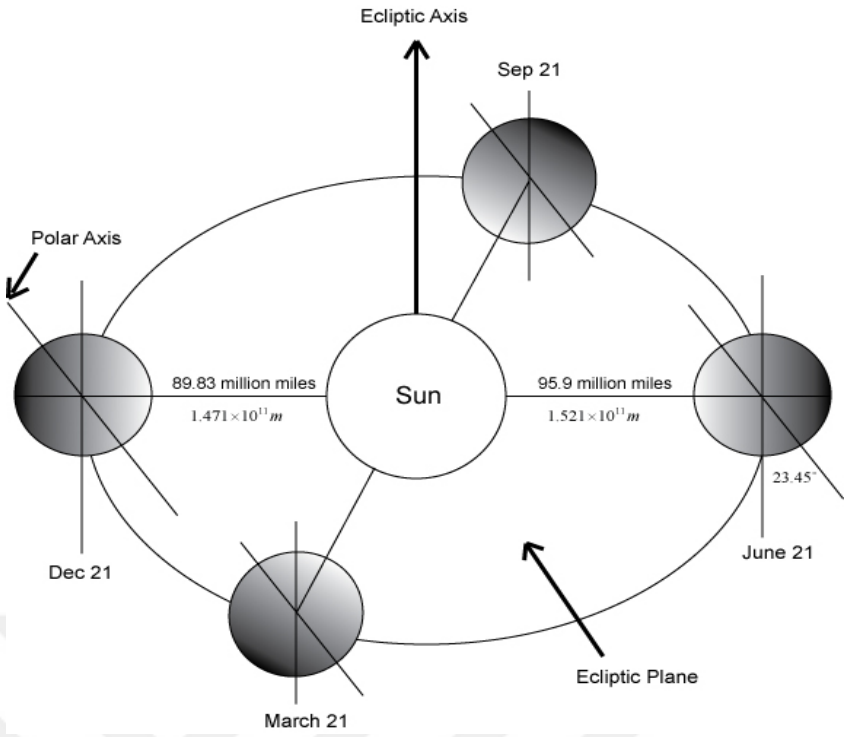

Figure 2.1: The tilt of the earth's axis.

2.2 Basic Earth – Sun Angles

The following angles could conclude and assert the position of a point as illustrated in figure (2.2) on the earth surface with regards to sun's ray at any given time.

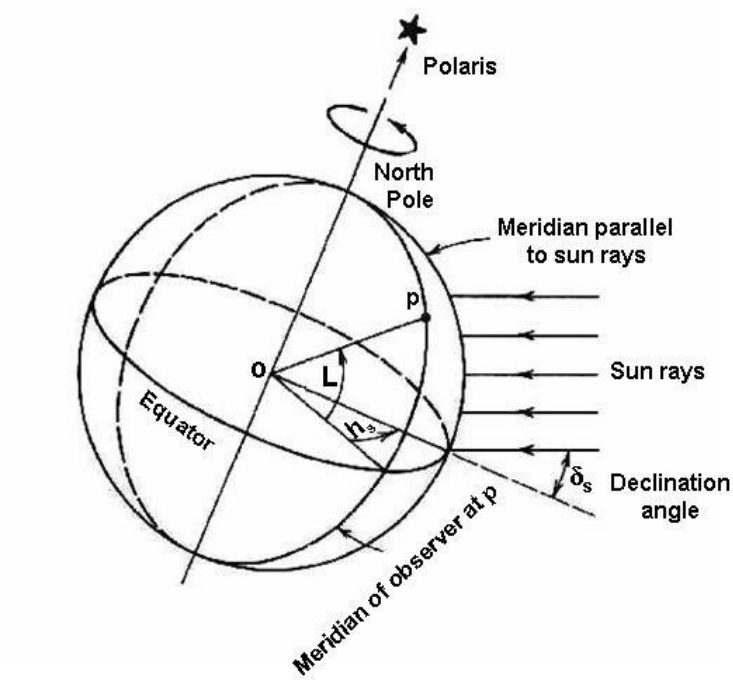

Figure 2.2: Basic earth- sun angles.

2.2.1 Latitude Angle (L)

This is known to be; the angular distance of the point (p) north or the south of the equator. It is the angle through which and between the radius vector *op* and its projection on the equator.

2.2.2 Hour Angle (hs)

This is the measurement in the plane of the earth equator that is positioned between the projection of the *op* and the projection of a line from the sun's center to that of the earth's center. The hour angle can be, therefore be illustrated and explained as follows:

$$h_s = 15\ (\mathrm{ST} - 12) \tag{2.1}$$

In the case where (ST) is solar time in hours, due to the earth's rotation (hs) varies at the rate of 150 per hour, which means that; (hs = 0) at solar noon [14]. For a clearer and better conversion of the solar time to that of the local time, the asserted knowledge of the location (longitude), the day of the year, and local standard meridian is required in details as shown in the following equation below [14]:

$$\mathrm{ST} = \mathrm{LST} + 4\ (L_s + -L_{10c}) + \mathrm{ET} \tag{2.2}$$

In the case where the (LST) is the local standard time, that the (LST) is the standard meridian for local time zone (45o for Baghdad), The (Lloc) is the longitude of location (44o for Baghdad), and then the (ET) is the equation of time in minutes and then it equals to:

$$\mathrm{ET} = 9.87 \sin(2B) - 7.35 \cos(B) - 1.5 \sin(B) \tag{2.3}$$

Where B, in degree is defined as:

$$B = 360\ (d_n - 81) / 364 \tag{2.4}$$

In the case where (dn) is the day number all throughout the year (1≤ d_n ≤ 365). There are, however, negative values of the hour angle east of due south (morning), on the other hand there are also positive values of the west of due to the south (afternoon) [14].

2.2.3 Sun's Declination Angle

(S_s) this is known to be the angular distance of a sun's ray, north (or south) of the equator. This angle represents a line that extends from the center of the earth to the center of the sun, and the projection of this line upon the plane of the equator. The angle of declination (S_s) is then therefore, estimated according to utilization of the following equation [15].

$$S_s = 23.45°\sin[360 * (284+ d_n/365)] \text{ degree} \quad (2.5)$$

2.2.4 Derived Sun – Earth Angles

Whereas in addition to the three (3) basic angles hour, the latitude and the sun's declination angles, numerous other angles are utilized to assert the position of the sun relative to the surface, this is now clearly illustrated in figure 2.3 [16]:

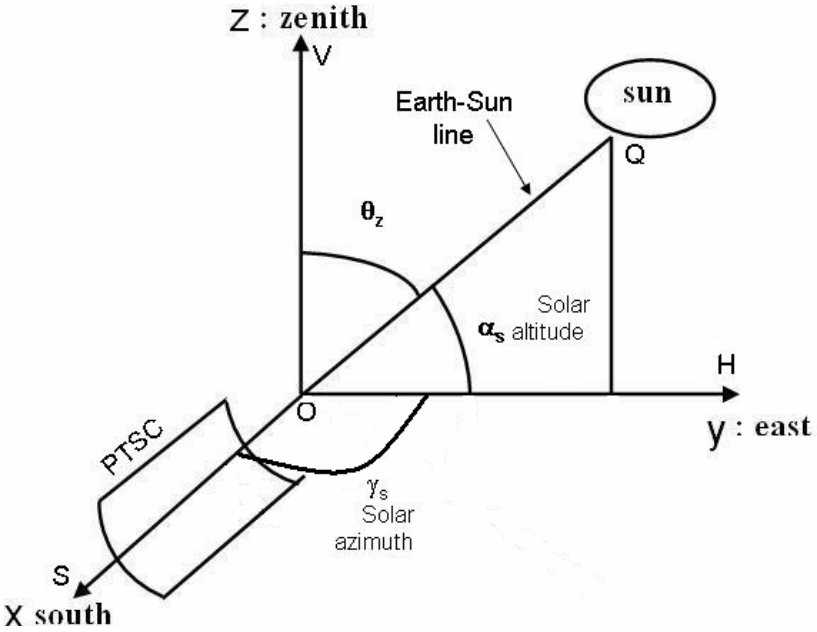

Figure 2.3: Derived sun – earth angles [14].

a. **Zenith angle (θ_2):** this is clearly known as the (angle QOV) between the sun's rays and a line perpendicular to horizontal surface at O.

b. **Solar altitude angle ($\propto_s$):** this is the angle QOH on a vertical plane between the sun's ray and its projection on the horizontal plane, i.e. the complement of the zenith angle. It is illustrated as:

$$\propto_s + \theta_2 = 90 \tag{2.6}$$

As can be calculated through the utilization of the following [17].

$$\sin(\propto_s) = \sin(S_s) + \cos(L)\cos(S_s)\cos(h_s) \tag{2.7}$$

c. **Solar azimuth angle (Y_z):** this is the angle HOS which it is the angular movement from the south to the horizontal projection of the rays of the sun. To ascertain the azimuth angle, the following equation can be utilized: [18].

$$\cos(Y_z) = [\sin(\propto_s)\sin(L) - \sin(S_s)/\cos\propto_s \cos(L) \tag{2.8}$$

2.3 Solar Radiation

The diameter of the sun is about 1.39 million km, it is a source of spherical radiation. Due to its enormous but finite size, it has an angular diameter of 0.53o (32') as shown in Figure (2.4). Solar radiation is a flow of energy coming out of the sun constantly and simultaneously in all directions. Solar radiation is a constant and simultaneous flow of sun energy in all directions. Solar radiation can be divided into two types, extraterrestrial and terrestrial [19].

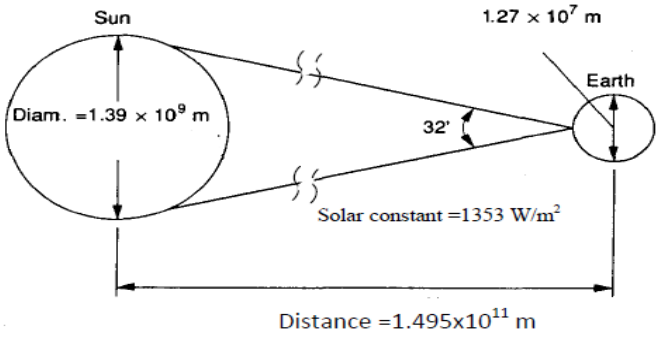

Figure 2.4: Sun-earth relationship [19].

2.4 Extraterrestrial Solar Radiation

The solar radiation outside the Earth's atmosphere is referred to as the extraterrestrial solar radiation (ETR) (Io). The ETR at the top of the Earth's surface relies on the numerous factors such as distance and orientation. ETR at the mean sun-to-earth distance, Dm is called solar constant, Isc was introduced for the first time by French scientist Pullet in 1837 [19] and the value currently accepted by NASA would be 1353 W / m2 the distance between the sun is 1.496.1011m. Due to the variation of the seasonal sun due to the Earth's elliptical orbit around the sun, the Earth-Sun distance varies by 1.7%. (Io) varies according to the inverse square law, as indicated in the following equation [17].

$$I_0 = I_{sc}[D_m/D_{e-s}]^2 \quad (2.9)$$

Where the De-s is the distance between the earth and the sun. there is then an ap

proximation of the value of (Io) for a given day of the year which can be found by utilization of the following empirically noted equation [19]:

$$I_0 = I_{sc}[1+0.034\cos(360d_n/365.25)] \quad (2.1)$$

2.5 Terrestrial Solar Radiation

There has always been a reduction in the amount of solar radiation that actually gets as high as the surface of the earth. This reduction occurs as a result of the reflection, the absorption and the diffusion of luminous molecules of gas stationed in the atmosphere. The total incident radiation on a surface (at the surface of the Earth) is composed of two forms: the first, the beam radiation, Ib, is the solar radiation on a surface having passed through the atmosphere without being substantially dispersed [19]. The second, which is the diffuse radiation, Id is the one that has reached the surface after being subjected to a significant diffusion by the atmosphere [19]. Global (total) radiation or terrestrial solar radiation is the sum of the beam and diffuse radiation [20]. Shah [22] gives a simple clear-sky model by Hottel [21] to predict the solar radiation of the beam at normal incidence, Ib:is indicated Shah [22]:

$I_b = I_0[\propto_0 + a_{1e}\text{-(KAM)}]$ (2.11)

The given and indicated Parameters (ao, a1) and (k) are empirical constants, and given by Duffie and Beckman [19].

$a_0 = 0.94[0.4237 - 0.00821\ (6- AL)^2]$ (2.12)

$a_1 = 0.98[0.5055\text{-}0.00595(2.5\text{-}AL)^2]$ (2.13)

$K= 1.02[0.2711 - 0.01858\ (2.5 - AL)^2]$ (2.14)

Where the AM is the air mass (Which equal to the $1/\cos\theta_2$ or $1/\sin \propto_s$) and AL, is the altitude of location above mean sea level (km). For tilted surface the beam radiation received is related to incident angle, θi given by [19]

$I_{bt} = I_b \cos \Theta i$ (2.15)

The Calculation of the diffused solar radiation on a horizontal surface can therefore be determined through the utilization of the following equation[14]:

$I_d = I_0 \cos \Theta 2[0.2710\text{-}0.2939(a_0 + a_{1e} - (KAM))]$ (1.16)

Important to notice that there is no effect of the diffused radiation on the layout of the concentrating collector calculation, however, there is a profound relevance of the fraction of direct radiation on the outcome and result of the focusing or on the concentrator collector.

2.6 Geometry of Parabolic Trough Solar Collector

The Parabolic Trough Solar Collector (PTSC) also referred to as the cylindrical parabolic collector utilizes the linear imaging concentration. These collectors are composed of the cylindrical concentrator of the parabolic cross-sectional shape accompanied with a receiver of the circular cylindrical shape which is along the focal line of the parabola. Figure (2.5) indicates a section of the PTSC.

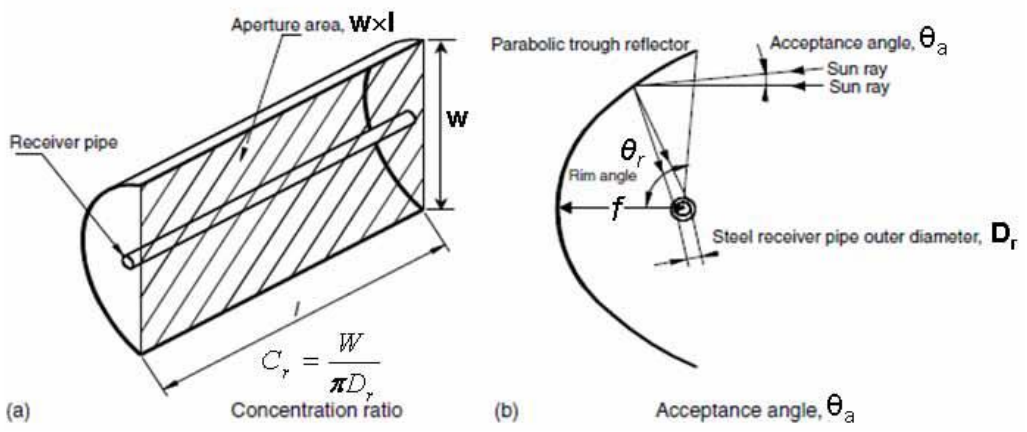

Figure 2.5: Cross-sectional view of PTSC [23].

While the Parabolic Trough Solar Collector (PTSC) utilizes the linear imaging concentration that are made up of a cylindrical concentrator of parabolic cross – sectional shape, and a circular cylindrical receiver which is located along the focal line of the parabola. A section of a PTSC is illustrated in figure (1-9). Technically it comprises of (1) a parabolic reflector, (2) an absorber (receiver) tube made of steel or copper coated with selective coating, and (3) a concentric tubular glass cover surrounding receiver with a gap of approximately 1-2 cm which is evacuated [23]. The cylindrical parabolic reflector pays a kin attentionon all the incident sunlight onto a metallic tubular or flat receiver placed along its length in the focal plane. The heat produces fluid that is permitted to flow out of the receiver. The parabolic reflector is controlled by its aperture diameter (W), rim angle (Θ_r), and the receiver's details both the shape and that of the size.

The "mirror radius", which is determined by the (r), is the radius of the parabola at an arbitrary place. So much so that the "radius of the rim" or the parabolic radius is the radius of the maximum mirror that then occurs on its outer edge. The angle of the rim then corresponds to the radiation of the beam reflected by the outer rim of the concentrator. The focal length, f, is related to the angle of the rim and the opening width W, as in [24]:

$$W = 4 f \tan[\theta_r/2] \quad (2.17)$$

The mirror radius at the point of incident of the beam radiation can ascertain the size of a reflected solar image at an accurate point. A simple equation for the image width *Wim*was advanced by Jeter [25].

$$W_{im} = \mathrm{r}\,\Theta_s \tag{2.18}$$

Now where (Θ_s)indicated the angular width of the incident beam radiation of 0.53°(≈ 0.00925 rad), with the acceptance half – angle $\Theta_a$of 0.267°, and the length of the path of the reflected beam which is clearly equal to the parabolic radius, (r). Hence, to a closely normal incidence, that occurs ina more frequent manner in the summer months, so the equation (1-8) may be rewritten as follows:

$$W_{im} = 0.00925\mathrm{r} \tag{2.19}$$

The geometric concentration ratio is indicated as follows [23]:

$$\mathrm{C}= \frac{Effective\ operation\ area}{Receiver\ tube\ area} = \frac{W - D_r 0L}{\pi D_{r0L}} \tag{2.20}$$

The concentration ratio (C) is known and recognized to be related to the (θr) which can also be referred to as [23]:

$$\mathrm{C}= \frac{\sin\Theta_r}{\pi \sin\Theta_a} \tag{2.21}$$

It is now clear to see that; the size of the receiver to that of the intercept of the entire solar image can be technically calculated. The diameter Dr of a cylindrical receiver is then; [19]:

$$D_r = 2\mathrm{r}\sin a = \frac{W \sin 0.267}{\sin\Theta_r} \tag{2.22}$$

For a flat receiver in the focal plane of the parabola the width W*f*is [19]:

$$W_f = \frac{2r\ \sin\Theta_a}{\cos(\Theta_{r\,+0.0267})} = \frac{W \sin 0.267}{\sin\Theta r \cos(\Theta r + 0.267)} \tag{2.23}$$

2.7 Optical Performance for PTSC

It is important to notice here; that there are numerous and distinctive effects that ought to be taken into further thoughts when utilizing the optical analysis of the solar collectors with that of the parabolic reflector, these outcomes, therefore include the optical properties of the materials, the relative size of receiver and the concentrator and of course notably the way of tracking and the corresponding losses.

2.8 Incidence Angle Modifier

Furthermore to the losses due to the angle of incidence, there are other collector losses that can be correlated to the angle of incidence. The magnification of the shifted images may result from errors in the concentration collector, tracking errors, as well as errors in the displacement of the focus receiver, which errors then affect the interception factor. These errors can be taken into account by the application of the incidence angle modifier K (θ_i) indicated and presented as an empirical fit to the experimental data for a given type of collector. The incidence angle modifier for the LS-3 manifold is [25,26].

$$K(\theta_i) = \cos\theta_i + 0.000884(\theta_i) - 0.00005369(\theta_i)^2 \quad (2.24)$$

Where the $(\theta_i,)$ the incidence angle, is provided in degrees

2.9 End Effect Correction

Some of the losses may therefore now surface at the ends of the receiver as, for a nonzero incidence angle, some of the length of receiver tube may not be illuminated by the solar radiation which is reflected by the mirrors.

Figure (2.6) illustrates the cases of how the end losses for an absorber with a nonzero angle of incidence [26]. For long collector strings, these end-effects are basically not relevant, so, in this research-study for the sake of shorter strings this may trivial due to the utilization of (2) two-axis solar tracking systems.

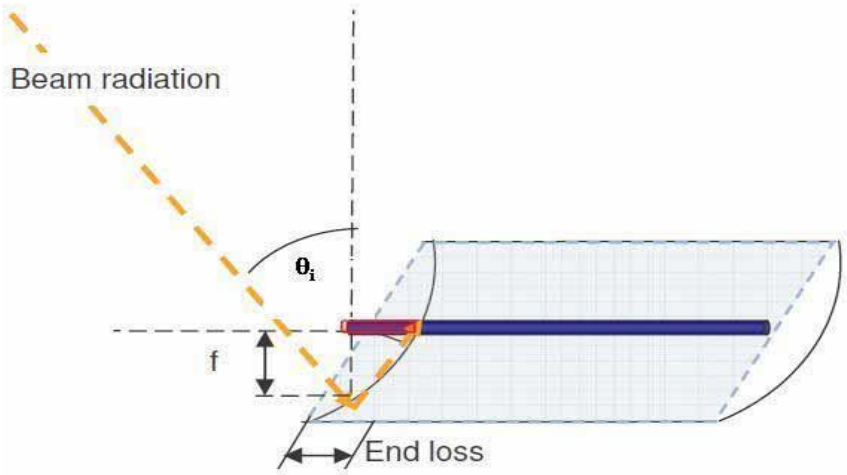

Figure 2.6: End losses from the receiver tube

The end losses XEND are the functional system; of the focal length of the collector, the length of the collector (L), and that of the incidence angle which is indicted through [26].

$$X_{END} = 1 - \frac{f}{L}\tan\theta_i \tag{2.25}$$

Therefore, the (2) two-axis solar tracking is expected to eliminate the end losses.

2.10 Optical Efficiency of the PTSC

The fraction of the solar radiation incident on the opening of the collector which is now absorbed at the surface of the receiver tube is referred to as the optical efficiency, η_0 [27].

$$\eta_0 = \frac{S}{I_b} \tag{2.26}$$

2.11 Thermal Performance and Losses of PTSC

In the case of the thermal conversion system, a working fluid can be used to achieve the same power from the receiver. The expectance of the thermal functional performance of the (PTSC) is brought about through their thermal efficiency which

is referred to as the ratio of the valuable power conveyed to the energy incident at the concentrator opening. The thermal losses for a PTSC are from the convection and radiation from the receiver tube to that of the ambient [23,28].

2.12 Heat Transfer to Fluid

The heat that transfers from the receiver tube to the fluid (HTF) ought to be characterized by the turbulent or the laminar flow conditions which accordingly, evaluates the Reynolds number, Re*f* of the fluid [30].

$$R_{ef} = \frac{4\,m}{\pi\, D_{r.i}\mu_f} \tag{2-27}$$

The Nusselt number of the fluid Nu*f*for laminar flow is indicated by the equation (1-29) and for turbulent flow by the equation (1-34).

If Re*f* <2200

$$N_{uf} = 3.7 \tag{2.28}$$

If Re*f* >2200

$$Nu_f = \frac{(f_f/8)\mathrm{Re}_f\,\mathrm{Pr}_f}{1.07+12.7\sqrt{(f_f/8)}[\mathrm{Pr}_f{}^{2/3}-1]} \tag{2.29}$$

Friction factor, *ff*, for smooth pipes is given by

$$f_f = ((0.79)\eta\,(R_{ef} - 1.64))^{-2} \tag{2.30}$$

The heat transfers of the coefficient, (hf,) to the fluid is then evaluated [30].

$$h_f = \frac{N_{uf}\,K_f}{D_{r.i}} \tag{2.31}$$

Where (m.,μ_f, $K_f$and Pr*f)* are mass flow rate, viscosity, thermal conductivity and that of the Prandlt number of the fluid, respectively. The (Dr,i) is the receiver inner diameter.

2.13 Overall Heat Transfer Coefficient and Factors

The overall heat transfer coefficient (Uo) is the coefficient for heat transfer from the surroundings to the fluid, based on the outer diameter of the receiver tube Dr,o, this is given by following equation [32,33]:

$$U_0 = [\frac{1}{U_L} + \frac{D_{r,0}}{h_f D_{r.i}} + \frac{D_{r,0}\, l_\eta [\frac{D_{r,0}}{D_{r,i}}]}{2K}]^{-1} \quad (2.32)$$

Where: The Receiver tube material's thermal conductivity is recognized as (K). It therefore becomes clear to assert an identity on the collector of the efficiency factor (F') as: the proportion of the really useful energy collected to the useful energy collected when is then the entire absorber surface which is at the mean fluid temperature.

$$F' = \frac{U_0}{U_L} \quad (2.33)$$

Now eq. 1-32 can be re-written in the following form [33]:

$$F' = \frac{1/U_L}{\frac{1}{U_L} + \frac{D_{r.o}}{h_f D_{r.i}} + \frac{D_{r.o}\ln(D_{r.o}/D_{r.i})}{2K}} \quad (2.34)$$

The heat removal factoror that of the correction factor, (FR), having a value between (0<FR<1), can be interpreted as the ratio of the actual useful energy which was collected to that of which would be collected if the all the whole absorbed surface was at the temperature of the fluid that went through the collector. The FR indicated a measure of the efficiency of the receiver when was however, viewed as a heat exchanger, in clear terms, the effectiveness by which the absorber radiation power was conducted to the running fluid. The working fluid flow rate and its

potentials were in addition to the thermal properties of the receiver material which technically controlled the value of the FR [34].

$$F_R = \frac{\mu' f C_p}{A_r U_L} [1- \exp (- \frac{A_r U_L F'}{\mu' f C_p})] \quad (2.35)$$

Where:

cp is the specific heat of the fluid.

The **co**llector flow factor F" is then described in the following equation:

$$Q_4 = \eta_o I_b A_a - U_L (T_r - T_{amb}) A_r \quad (2.36)$$

2.14 Thermal Efficiency of a PTSC

The calculation of the spontaneous thermal efficiency Ηth of a solar concentrator can be obtained and achieved through the energy balance on the receiver. The convenient gain of heat, Qu, provided by the receiver could be illustrated in terms of the optical and that of the thermal losses, such as the optical losses which were been expressed by the optical efficiency, η_o [23,35].

$$Qu = \eta_o I_b A_a - U_L (T_r - T_{amb}) A_r \quad (2.37)$$

Now where Aa is the aperture area, as the temperature of the surface which is quite difficult to measure, it is important to indicate that the Qu in terms of the temperature of the inlet fluid by measures of heat removal factor (FR) is given as follows [36]:

$$Qu = A_a F_R [S - \frac{U_L (T_{f,i} - T_{amb})}{C}] \quad (2.38)$$

The valuable heat is therefore related to the flow rate which can also be referred to as the base of the fluid difference temperature as [23]:

$$Q_u = m' C_p (T_{f,o} - T_{f,i}) \quad (2.39)$$

Where: (Tf,I) indicates the inlet fluid, then (Tf,o) illustrates the exit fluid and (Tamb), that of the ambient temperatures.

The thermal efficiency of the solar thermal collector can also be simplified and acknowledged as the ratio of valuable heat (Qu), which was delivered per Aa, and the insulation, Ib, which was incident on the aperture.

$$\eta_{th} = \frac{Q_4}{A_a I_b} \tag{2.40}$$

The thermal efficiency of the collector then can now be stated again from the eq. 38 and eq. 40 as follow [36,37]:

$$\eta_{th} = F_R[\eta_o - \frac{U_L(T_{f,i} - T_{amb})}{I_b C}] \tag{2.41}$$

The thermal efficiency relies on the (2) two types of quantities which are mostly the concentrator design parameters and then that of the parameters grouped in the operating conditions. The design dependent parameters which included the optical efficiency, heat loss coefficient and that of the heat removal during the opening requirements that couldbe referred to as the solar flux, inlet fluid temperature and the ambient temperature [23].

The exit fluid temperature, (Tf,o) and that of the temperature rise, (Tf,o-Tf,i) and the efficiency which could be calculated through the utilization of the following equation [23,37].

$$\eta_{th} = \frac{m' C_p (T_{f,o} - T_{f,i})}{I_b A_a} \tag{2.42}$$

2.15 Literature Review

Noticeably various studies have been conducted and the absorption tube efficiency has been enhanced. Eight studies will be listed including but not limited to:

2.15.1 Y. Aldali1,2, T. Muneer1 and D. Henderson1

A CFD simulation was performed in order to compare (w) containing the distinctive internal helical fins. In this research study, the various sizes of pipes (100, 200, 400 mm) were utilized and this showed to be the 100 mm. The results showed that the usage of helical fins in the tubes provides the good results in the comparison with tubes that have no fins, signifying that more thermodynamic distribution is channeled out on the tube instead of heat concentration in the lower half of the tube [38].

2.15.2 Javier Mu.oz, Alberto Ab Nade

As derived from his research and his analysis of the effect of the use of internal finned pipes for the design of equivalent stone complexes with the study of fluid dynamics. We have suggested a group of tube configurations comparing them with a reference commercial tube. Our analysis shows how the parasitic losses associated with pressure loss in the tube will increase with the number of fins and their snail angle. On the other hand, thermal losses are reduced resulting in an increase in thermal efficiency and vitality of the collector [39].

2.15.3 Cheng Z.D et al (2012)

This research-study turbulent flow and coupled heat transfer enhancement in trough solar absorber tube. The outcomes of the Reynolds number, heat transfer fluid (HTF) inlet temperature, and incident solar radiation and LVG geometric parameters were further examined. It has been discovered that there is a drop of both the average wall temperature and the thermal loss as the Reynolds number rises. Furthermore, as there is increment in the incident solar radiation, both average wall temperature and the thermal loss will increase. The figure 2.7 below indicates the results of LVG parameters on $q_{lost.}$ [40].

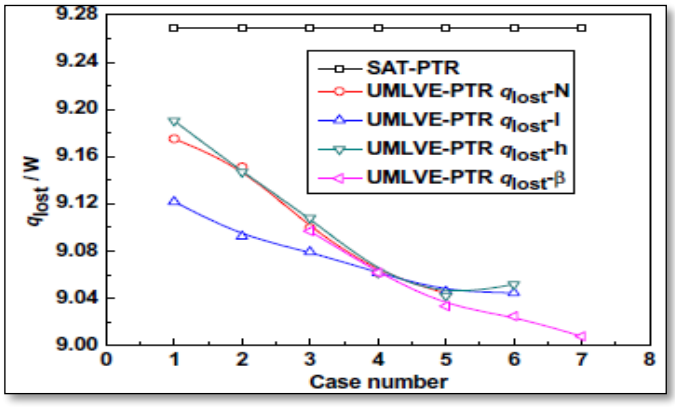

Figure 2.7: Effects of LVG parameters on q $_{lost}$ (Cheng Z.D et al2).

2.15.4 P. Wang a,b, D.Y. Liu a, C. Xuc

The current study examines the outcome of inserting metal foams into receiver tube of parabolic trough collector on heat transfer. Realistic non-uniform heat flux boundary and the measured physical properties of metal foams are employed to describe the heat transfer characteristic accurately in superheated. In general, adaptability and superiority of inserting metal foams at superheated segment of the (DSG) system suggested by this study can be anticipated as follows: (a) Lowers the drop of pressure when metal foams are inserted. (b) Reduces the difference of circumferential temperature in order for extending the life of receiver tube. (c) Enhances efficiency of heat transfer in order to shorten the length of superheated section. The figure 2.8 below illustrates the temperature distribution on the out surface of receiver tube [41].

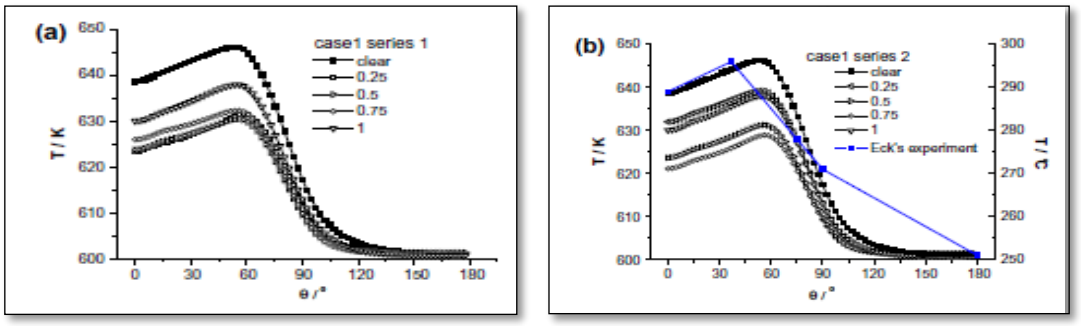

Figure 2.8: (A),(B). Temperature distribution on the out surface of receiver tube.

2.15.5 Almanza, R. *et al. Solar Energy,* 1998

Different experimental conditions have been set up to examine the receiver behavior of parabolic troughs in direct steam generation (DSG). When cool water was fed into steel receiver pipes (0 = 2.54 cm), the pipes deflected. This bend advanced like a wave from the inlet to the outlet end, with deflection of about 6.5 cm at the centre of each section (2.90 m long) in the parabolic trough module (14.5 m long and 2.5 m aperture). This resulted from a difference in temperature of about 50°C in the circumferential direction. When a copper receiver was used instead of a steel one, the circumferential temperature difference was practically eliminated and no appreciable bending of the pipe was observed. The (DSG) was thus obtained without these problems [42].

2.15.6 Vicente Flores, Rafael Almanza

Based on this study a bimetallic Cu–Fe receiver has been proposed for use in the (DSG) at low power generation. They try to understand how such a receiver can work under stratified two-phase flow regimen forms, also they try to establish the technical feasibility of using the (Cu–Fe) wall receiver in parabolic troughs concentrators. This study has been conducted for the (DSG) at low power output. If beam radiation reaches the one end of the receiver more than on the other end, a more extreme deflection will occur. The (2) experiments and the mathematical model revealed that such results. It can be concluded mainly that a bimetallic absorber is possible to be used with (DSG) under any direction of the beam radiation. As only a small deflection is generated in such as absorber, the glass envelope will not be broken [43].

2.15.7 Delussu G.2012

An extensive qualitative on a standard solar pipe receiver has been conducted for improving heat distribution around the pipe. It has been revealed that there is good effect of roughness on distribution of temperature, however it increases the viscous losses [44].

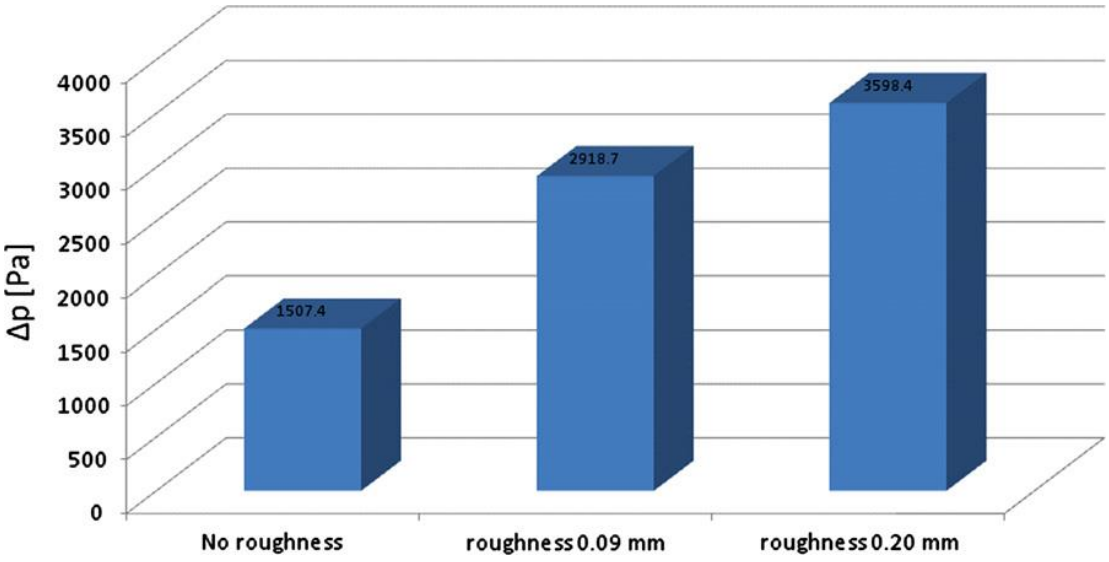

Figure 2.9: Effect of adding roughness on the pressure drop. The pressure drop is plotted for the standard smooth pipe.

2.15.8 WANG Kun, HE YaLing & CHENG ZeDong. 2014

In this investigation work, using a secondary reflector as a homogenizing reflector (SR) in a classical parabolic trough solar collector (PTSC) was suggested to homogenize the solar flux distribution, thus increase the dependability of the PTR.

By adopting the Monte Carlo ray-trace (MCRT) the design manner of this type PTSC with a SR was also proposed. Meanwhile, the flux distribution of concentrated solar was calculated approach. After that, the incorporate heat transfer process in the PTR was simulated by handling the solar flux calculated by the MCRT model as the heat flux condition for the limited volume method model. The solar flux distribution on outer surface of the tube, the temperature scope of the absorber tube wall, and the collector efficiency in detail. It was detected that the absorber tube could approximately be heated uniformly in the PTSC with a SR. Afterward, both the circumferential temperature difference and the maximum temperature can be reduced markedly, even so, the efficiency tended to drop slightly as a result of the inevitably increased optical loss. Under the conditions examined in this study, even though, despite the fact that the reflector efficiency declined by about 4%, the circumferential temperature difference was minimized from about 25 to 4 K and the extreme temperature was lowered from 667 to 661 K. The figure 2.10 below shows temperature distribution on the absorber tube wall. (a) Before improvement and (b) after amendment [45].

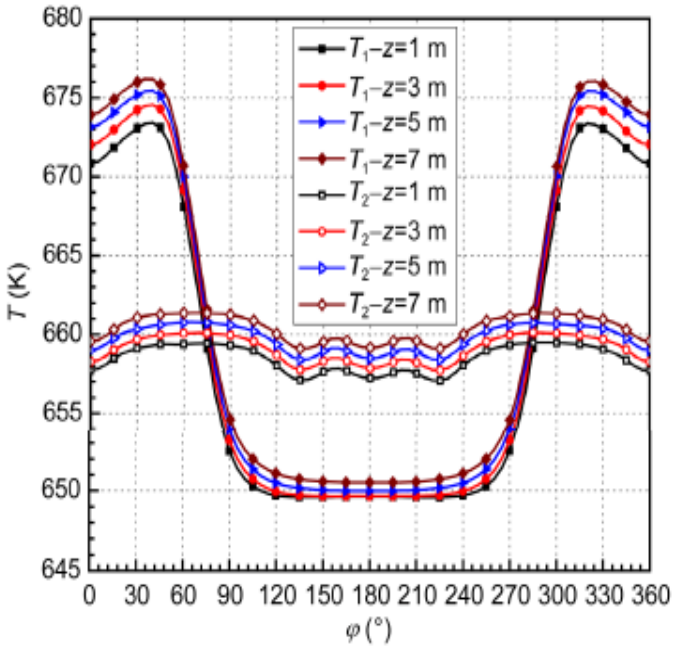

Figure 2.10: Distribution of circumferential temperature at different axis locations.

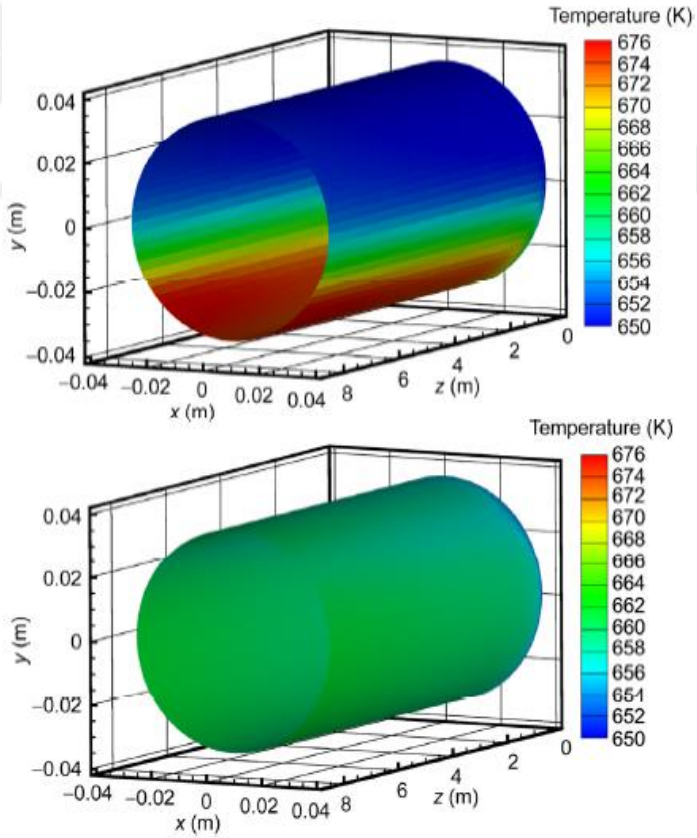

Figure 2.11: Distribution temperature on the absorber tube wall. (a) Before improvement and (b) after improvement.

2.15.9. Wolfgang Spirkl, Harald Ries, Julius Muschaweck and Andreas Timinger. Received 18 December 1996; revised version accepted 23 May 1997.

Compact secondary concentrators have been suggested which are built up in agreement with the principle of edge ray; they are consisted of an in volute part and an edge ray reflector with a form closely resembles a straight line. Using these reflector forms as a starting point. The total concentration with these secondary concentrators reaches 77% of the theoretical upper limit for a pill box solar distribution. An optimized involutes only secondary reflector yields a concentration of 60% of the theoretical maximum, whereas the concentration without secondary is only 46% Therefore, the secondary concentration under these conditions is 0.77/0.46=1.7 [46].

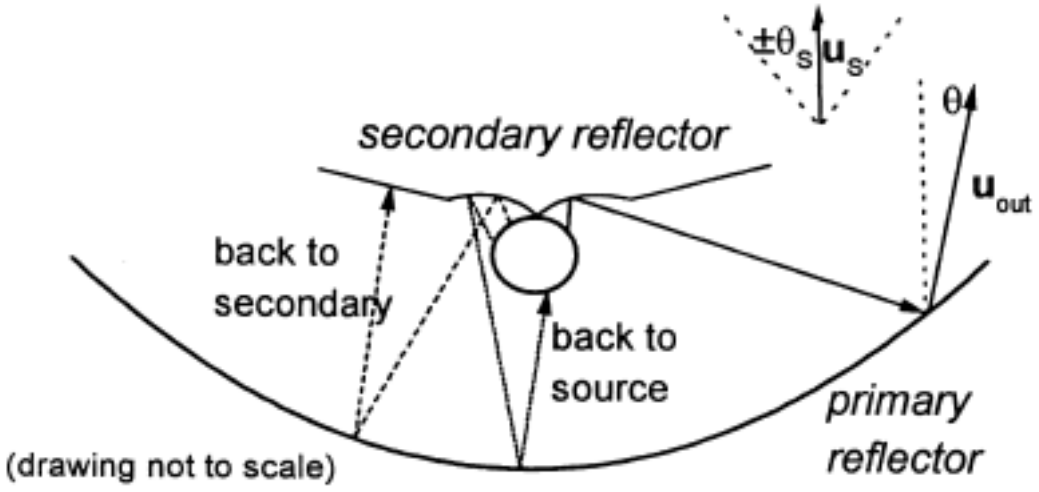

Figure 2.12: The broken lines correspond to rays which are reflected back to the absorber or to the secondary reflector.

CHAPTER THREE

METHODOLOGY AND EXPERIMENTAL PART

3.1 Introduction

This work focuses on a new design and fabrication of PTSC system practically to overcome the failures resulting from the high temperatures resulting from the reflection of solar radiation on the absorbent tube, also benefit of largest amount incoming of solar radiation to convert it thermal energy, that is by helping the secondary reflector (SR). This chapter contains a description of Parabolic Trough Solar Collector (PTSC), in addition the new part (secondary reflector) and a detailed explanation of how the components of the device work. The design of the system was conducted at the industrial city (Ostom) in Ankara, and tests of the system was conducted in yard of University of Turkish Aeronautical Association.

3.2 Description of The Parabolic Trough Solar Collector with The Secondary Collector

Before addressing to the trough collectors design details, it is important to mention the place of the trough in the University. The place chosen is located next to the mosque inside the Turkish Aeronautical Association University. There was a restricted space for the system that is outlined by a buildings because of the university requirements which were to leave a enough distance to the cars and buses to arrive their destination to and from behind the university. Building, and also the system was not allowed to be placed on the grass and had to be a certain distance away from the airport's runway.

A small model has been tested in the open area of the university of Turkish aeronautical association. This model consisted of fixed base with moveable base

Installed on it the reflector, absorber tube and secondary reflector the newly developed PTSC-SR as shown in figure (3.1). Specifications are given in:

Table 3.1: Specifications of PTSC-SR

ITEM	Value/Type
Aperture length	1m
Aperture width	60cm
Receiver diameter	22mm
Tracking mechanism type	Manually
Mode of tracking	One- axis
Type of the reflector materi (main reflector-secondary reflector)	Stainless Steel
Length of secondary reflector fin	3.2cm
angle of secondary reflector	130°
Rim angle	69°
Thickness of the absorber	2mm
Concentration ratio rate	8.7

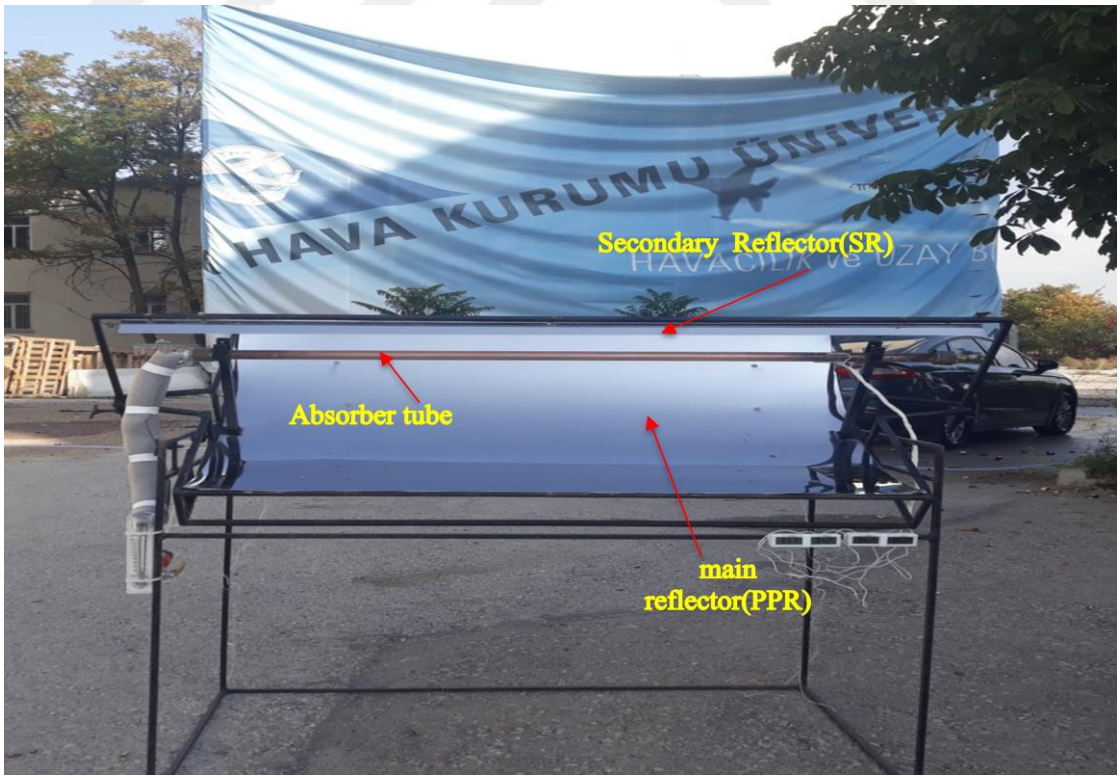

Figure 3.1: Parabolic trough solar collector (PTSC) with secondary reflector (SR).

3.3 System Components

3.3.1 Fixed Part

It is base made of iron, it has been made to withstand the weight of the moving base and its accessories, also to withstand weather conditions.

3.3.2 Movable Part

The part on which the main reflector is installed, absorber tube and the secondary reflector. This base has been designed in order to has an axial movement for tracking the sun rays manually, also this base made of iron as shown in figure (3.2).

Figure 3.2: Moving part.

3.3.3 The Main Reflector (PPR)

This reflector made of stainless steel and has a high ability to reflect solar radiation very well, it has ability to resist bending, breaking and weather conditions. Reflector length 100 cm, width of aperture 60cm as shown in figure (3.1).

3.3.4 Absorber Tube

This tube made of copper, diameter 22 mm, the length 90 cm. Copper was selected for its ability to absorb the solar radiation (heat) quickly, especially in this work we did not use the glass cover in order to get precise temperatures on the tube wall while performing experiments.

3.3.5 The Secondary Reflector (SR):

A small scale reflector made of stainless steel too, It has two ribs, the length of each side is (3.2 cm) and the angle between ribs is ($130^{O}C$) as shown in figure (3.1).

3.3.6 Thermocouple

In these experiments we used six thermocouples, four thermocouples measure the temperature changes on the surface of the absorption tube (four points), a thermocouple to measure the temperature of the water entering the absorption tube, thermocouple to measure the water temperature coming out of the absorption tube as shown in figure (3.3). Table (3.2) shows the characteristics of the thermocouple:

Table 3.2: characteristics of the thermocouple.

	Specification	
1	Measuring temperature rang	-50 – 100 ^{O}C
2	Temperature accuracy	$\pm$ 1 ^{O}C
3	Temperature display resolution	0.1 ^{O}C
4	Operating voltage	1.5 v
5	Dimension	48x28x15.2 mm

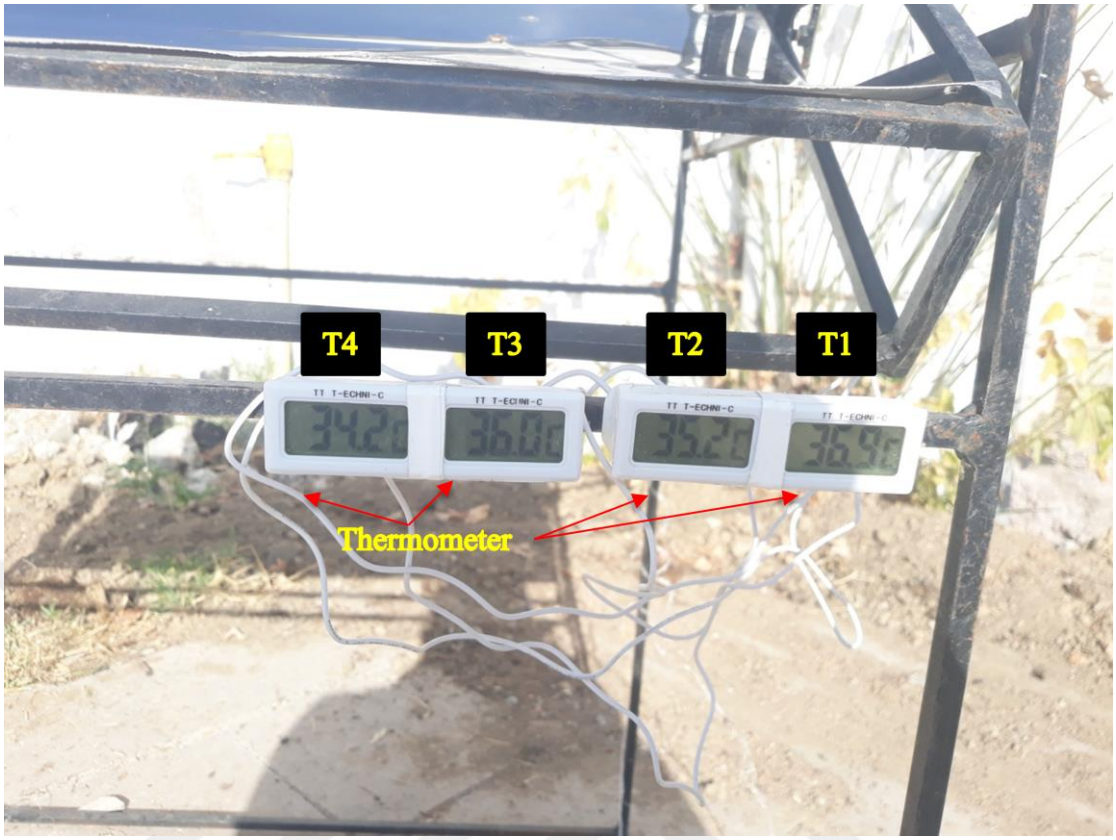

Figure 3.3: Temperature thermocouples for the absorber tube.

3.3.7 The Flow Meter

It is a device for measuring the volumetric flow rate of water entering the absorption tube and controlling the flow rate as shown in figure 3.4 (a), (b).

This flow meter has many characteristics which are listed below.

1-High accuracy.

2-Easy to read linear scale.

3- Direct reading.

4- does not need to flow straightened or requires special Pipes.

5- Install in any position.

Figure 3.4: The flow meter- front view and side view.

3.4 PTSC and PTSC-SR

The conventional PTSC system consists of: Parabolic trough collector and the absorber tube (receiver AT) as shown in Figure (3.5).

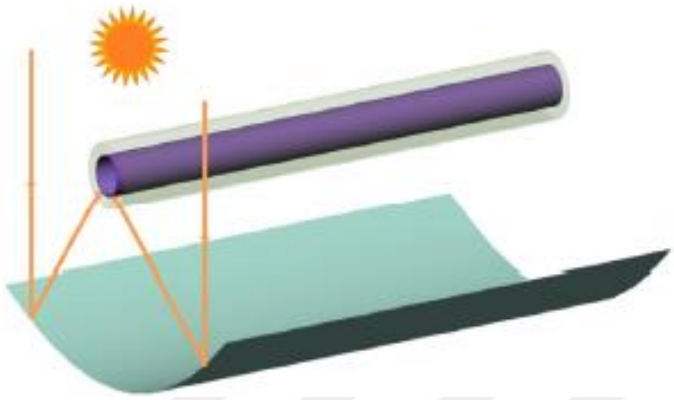

Figure 3.5: Conventional PTSC.

The absorber tube is positioned along the focal line of the parabolic trough concentrator to receive the concentrated solar energy which is fundamentally reflected on the bottom points of the absorber as shown in Figure (3.6). To homogenize the distribution of solar flux on the absorber tube surface, the following modifications on the conventional PTSC are as a next:

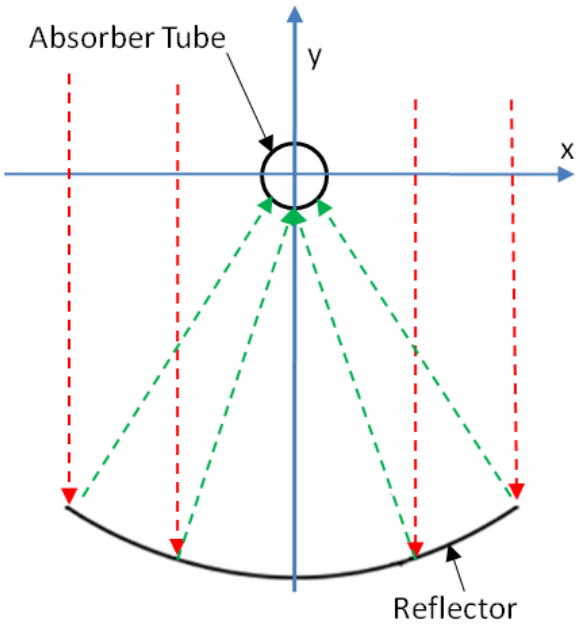

Figure 3.6: Solar reflection in conventional PTSC.

1- The absorber tube is moved down to a appropriate position from the focal line of the parabolic trough concentrator to allow a beam of the reflected radiation to pass to the secondary reflector (SR).
2- Addition the SR. The SR and the parabolic trough concentrator are arranged in such a method, that their aperture is opposite, as shown in Figure (3.7).

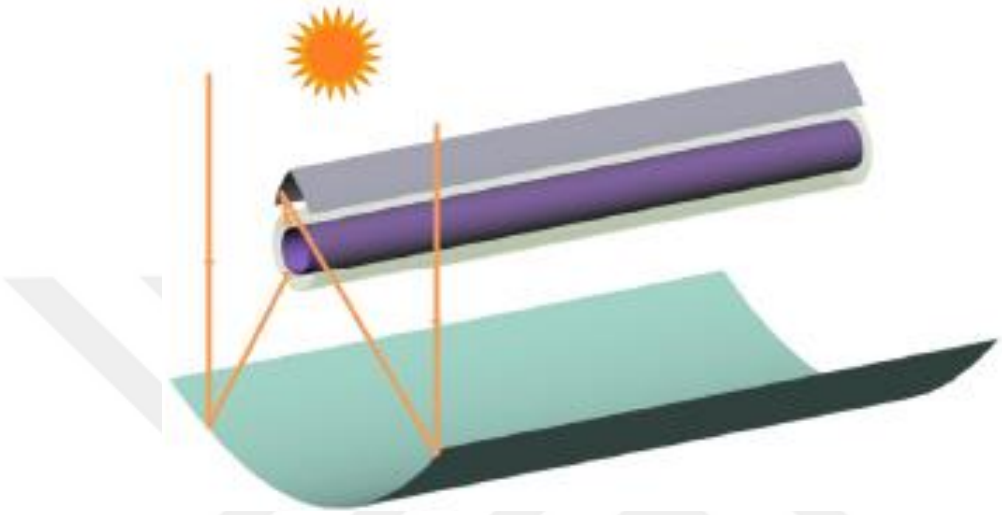

Figure 3.7: Conventional PTSC with SR.

3.5 Design Concepts for the Reflecting Parts Assembly

The reflector is designed to set the focal length (f)is

22 cm from the vertex (V), the aperture width of the system (W) is 60 cm so the equation of the designed system will be

$$x^2 = 0.88y \quad (3.1)$$

determine the Focal length (f) by this equation below

$$f = W/4 \tan[/\varphi r/2] \quad (3.2)$$

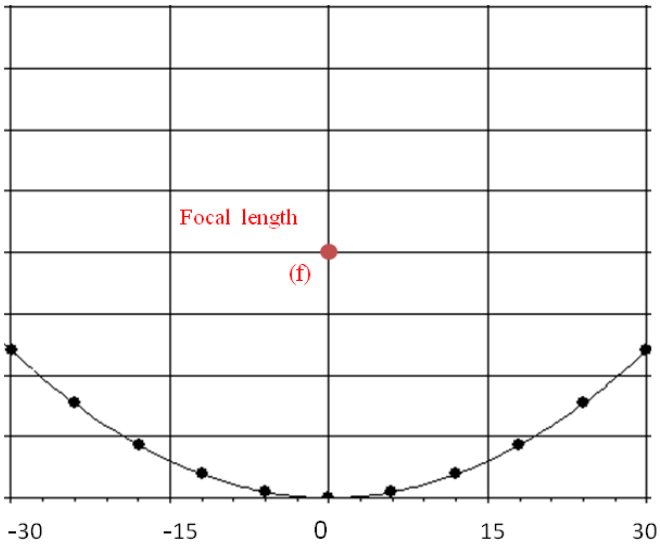

Figure 3.8: Basic design of the PTSC.

3.6 The Working Notion

In the PTSC with a SR, a part of the solar rays are reflected directly by the main reflector and concentrated onto the bottom surface of the absorber tube. The other rays are reflected onto SR surface by the main reflector, then reflected again by the SR onto the top surface of the absorber tube. Thus, uniformly the solar flux is distributed on the entire surface of the absorber tube almostly, as shown in Figure (3.9). During the design process. There are two main things, that is placement the location of AT and determine the SR, we have done the following.

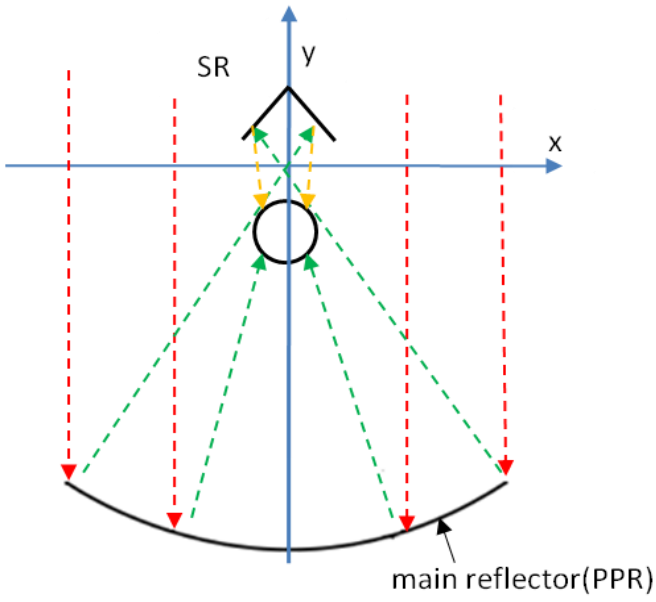

Figure 3.9: Solar reflection by PTSC-SR.

3.7 Dividing the PPR Surface

The coordinate system is established on the focal point of the main reflector cross section, as shown in Figure (3.10). Two equal points C1 and C2 on the main reflector surface are selected arbitrarily. The main reflector is divided into three parts by the two points: the FC2 part, the EC1 part, and the C1C2 part. The rays reflected by the C1C2 section of the main reflector surface are required to be concentrated on the bottom surface of the absorption tube, while the rays reflect by the (EC1, FC2) sections, to reach the SR surface and then reflected again on top surface of the receiver.

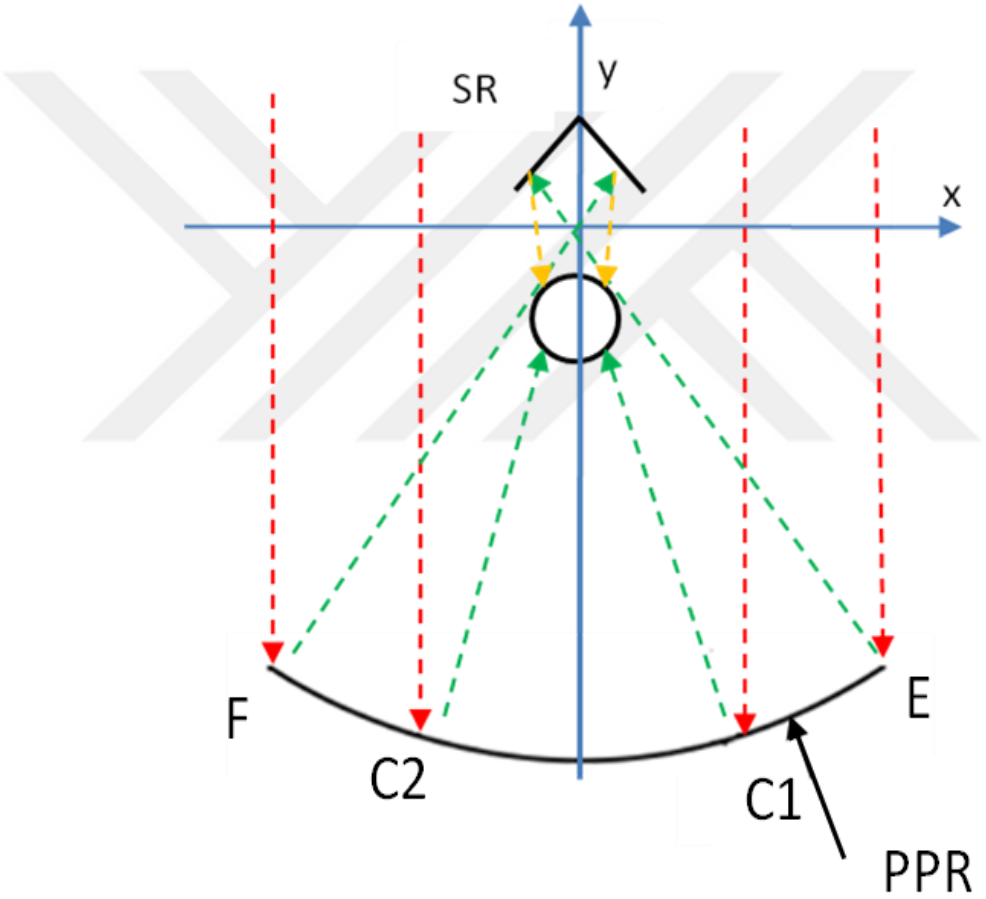

Figure 3.10: Determine the reflection points when designing.

3.8 Determine (RT, SR) Positions

At this stage, it was gradually lowered the absorber tube (AT) to allow the part of the reflected radiation from the main reflector (PPR) to pass up to the top to meet with the secondary reflector (SR), we have been lowered the tube absorption gradually until we get the best location (the right place to receive the reflected radiation from PPR). At the same time, we moved the secondary reflector (SR) up and down until we have got a suitable position that could reverse the solar radiation coming from the main reflector (EC1-FC2) and then reflected again on the top surface of the absorber tube. In this figure (3.11) the diagram shows the complete steps for the PTSC-SR.

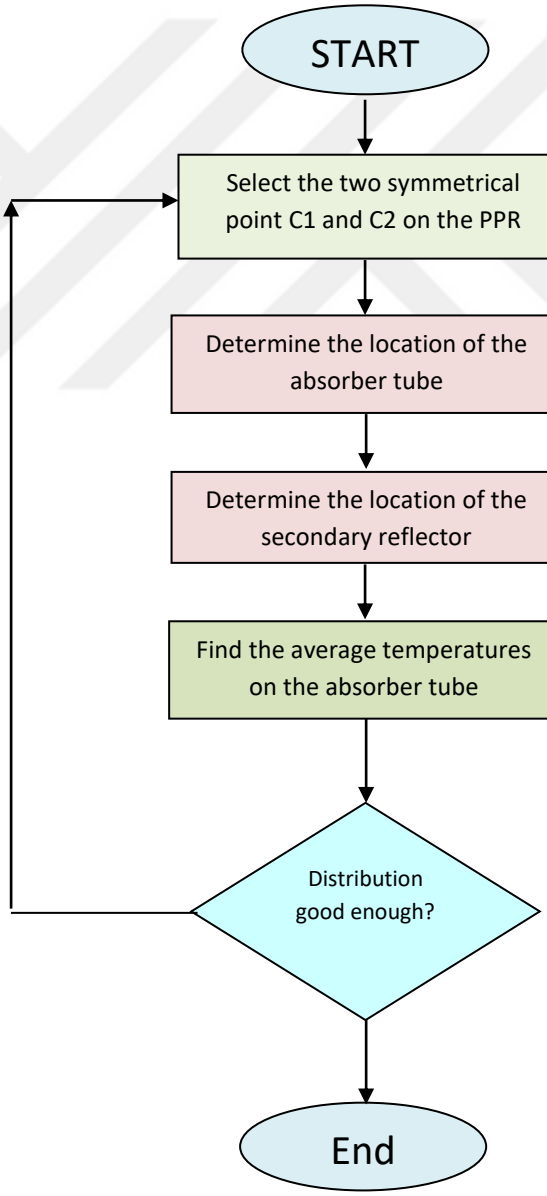

Figure 3.11: The diagram shows the complete steps for the PTSC-SR.

3.9 The Experimentation

Two of the experiments done, first one on the conventional parabolic trough solar concentrator (PTSC), and second one after addition the secondary reflector (SR), were the same as the weather conditions. First of all, we assembled all the parts of the device, which is consists of the pump, the thermometers, fixed base, movable base, the main reflector (PPR), absorber tube and the secondary reflector (SR), then we connected the water source from the pump to the liquid meter to determine the quantities of water entering the absorption tube. Four readings has been entered (the same readings were applied in the first experiment and the second experiment to compare between them), after the water is out of the fluid meter and entered into the absorption tube, the water obtained the heat through cross the absorption tube. Before leaving the water, we installed four thermometers at four points at the end of the absorbent tube (top, bottom, right side and left side) to see the difference in changing temperatures each time. Results were taken and data recorded and there were slight differences in temperature depending on weather conditions. We will know these results in the results chapter.

CHAPTER FOUR

RESULTS AND DISCUSSION

4.1 Introduction

In this chapter, investigation of the parabolic trough solar collector (PTSC) with the secondary reflector is presented. Thermal performance of PTSC (for the first and second parabola) are also evaluated by using the measurement the temperatures of flow rate, heat transfer fluid (water) for inlet and outlet, ambient temperature, wind velocity, and the global solar radiation.

The test was conducted at Turkish Aeronautical Association University, Ankara on August, 2018 from 1.00 pm until 3:30 pm, and data were recorded with a time period approximately 30 minutes. Also in these experimental work will draw graphically the parameters of inlet and outlet temperatures with thermal efficiency and heat gained and demonstrated in details, then comparisons between experimental works.

Note: On the first experiment we performed tests on (PTSC) without secondary reflector (SR), on the second experiment the tests were using the secondary reflector.

4.2 Changing the Ambient Temperature and Wind Speed During Experiments

The ambient temperatures and wind velocity were differentiated throughout the test days. The parameters did not measured experimentally, only the data were taken from an online source [39], at the beginning the testing day, The ambient temperature was low compared to the mid- period of working, it starts increasing with the time goes until it reaches a maximum value of 32°C approximately from 1:30 P.M to 3:30 P.M. Then, slightly it decreases at the end of the experiment, until arriving to 30°C at 4:00 PM. Wind speed readings were taken from 10 to 15 km/h. At the beginning of

the experiment, the minimum reading was 10 km at 12:30 PM and began to increase until 15 km/h at 16:00PM.

on the second experiment (use of the secondary reflector), temperatures were close to the previous day with high wind speed. The temperature was at the start of the experiment 32.9°C at 12:30PM and reached 34.2°C at 2:30PM and then began to drop until it reached 32.7°C at 14:30PM.

The wind speed on this working day was faster than the day before. At the beginning of the work, the wind speed was 19 km/h at 12:45PM and began to decrease over time until it reached 16 km/h at the end of the work.

4.3 Inlet and Outlet Temperature

In this section, we will display the inlet and outlet temperatures of PTSC and PTSC with secondary reflector (SR).

4.3.1 Inlet and Outlet Temperatures (PTSC)

Figure (4.1) shows the input and output temperatures of PTSC throughout experiment period. At the beginning of the experiment at 1:00PM the temperature of the water has begun to rise, this increase in temperature continues slightly until about 2:00PM and then is almost constant and reached the highest temperature of 28.1°C at the entry of water and 28.8°C at the exit of water at 2:30PM. At 3:00PM the temperature starts to gradually descend until it reaches the lowest level, 26.9°C at 3:30PM. As seen in table (4.1). Temperatures expected to be bigger than this range, this is because the glass tube is not used in this experiment, in addition, we did not use sufficient insulation to protect the water heat loss passing through the tube from the water source to the device. In these data above has been used the flow rates of 3.5, also in the second experiment.

Table 4.1: Difference in temperature for entry and exit (PTSC).

Time(h)	At enter the water (°C)	At exit the water (°C)
1:00	26.2	26.8
1:30	27.1	27.8
2:00	27.7	28.5
2:30	28.1	28.8
3:00	27.8	28.3
3:30	26.9	27.4

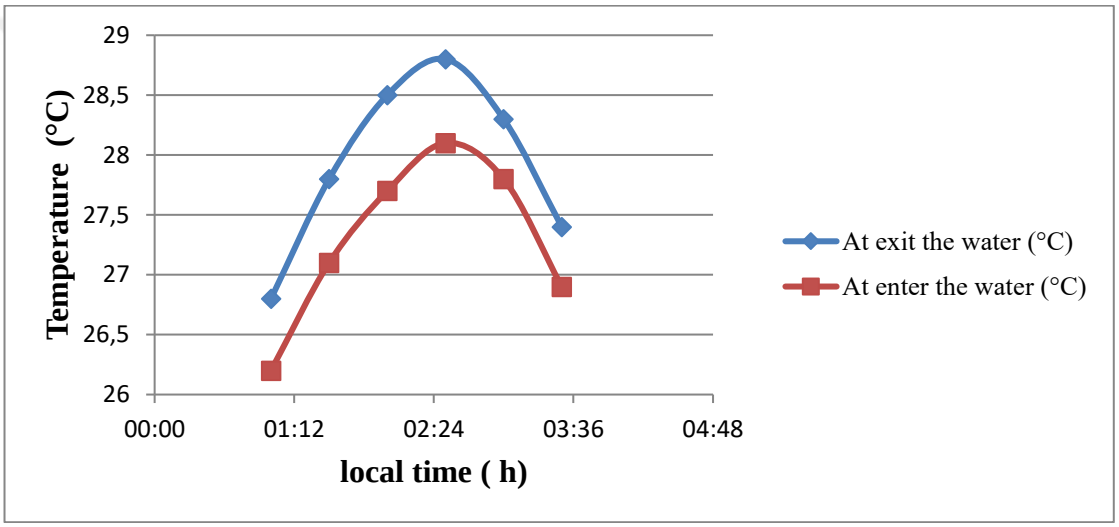

Figure 4.1: Inlet and outlet temperatures of (PTSC).

4.3.2 Inlet and Outlet Temperatures (PTSC) with (SR)

On this tests day, inlet and outlet temperatures of (PTSC –SR) during the working period temperatures were relatively high compared to the first day of tests, which was 34.2°C (2.2°C higher than the first day). Also the wind speed was faster, reaching 19 km/h, and this may lead to loss insignificant temperatures. As it was under the conditions of the first experiment, the temperatures at the beginning of the experiment are as low as possible and continues to increase until reaching the highest level of 27.2°C at 2.5 PM, may be the delay time in the high temperature in this experiment because of different wind speeds. The temperature of the liquid starts

decreasing at the end of the experiment, reaching to 26.3 at 3.30PM. The figure (4.2) and table (4.2) below illustrate the above

Table 4.2: Difference in temperature for entry and exit (PTSC-SR).

Time(h)	At enter the water (°C)	At exit the water (°C)
1:00	25.3	26
1:30	26	26.8
2:00	26.8	27.8
2:30	27.2	28.1
3:00	26.9	27.7
3:30	26.3	26.8

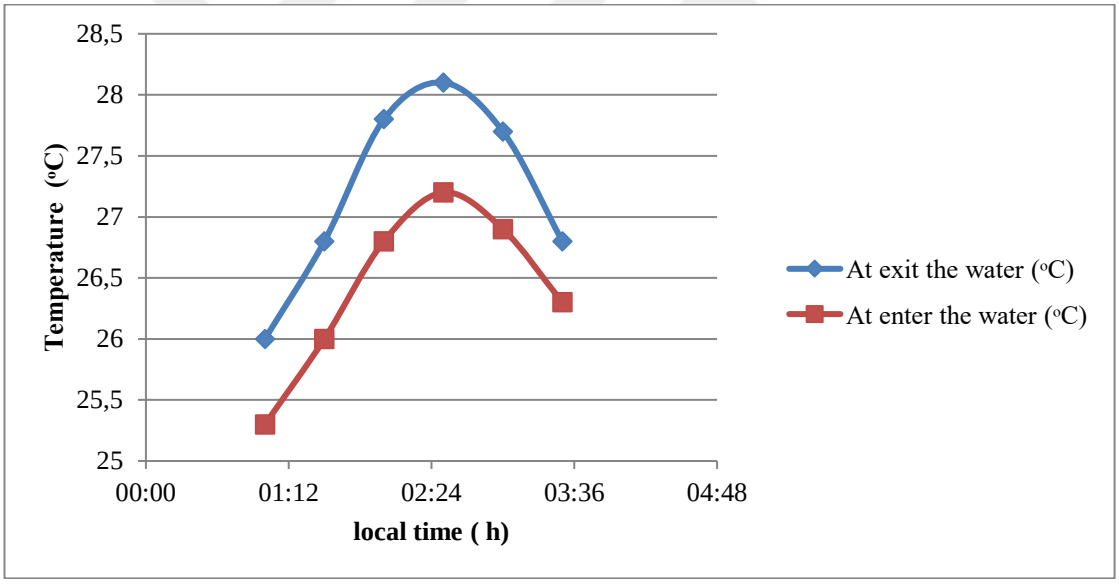

Figure 4.2: Inlet and outlet temperatures of PTSC-SR.

4.4 Determination of Thermal Distribution on the Outer Tube Wall

In this experiment, the thermal distribution was determined on the outer surface of the absorption tube by placing four points, shown in figure (4.3), to measure the temperature of the absorption tube, called T_1, T_2, T_3, T_4.

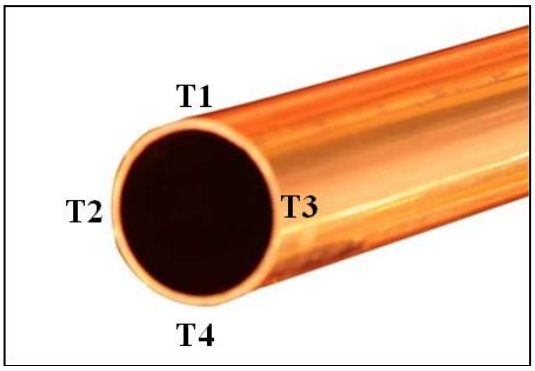

Figure 4.3: Shows the main points of temperature measurement points on the tube.

4.5 Temperature Measurement with Different Flow Rates

In these tests, the difference in temperature was measured with different quantities of water flow inside the tube as shown in Table (4.3) and figure (4.4) below. This experiment was performed on PTSC and PTSC with SR. These results will show the difference of solar radiation distribution on the absorption tube in both cases.

Table 4.3: Temperature for each point with difference Q (PTSC).

PTSC					
Time/h	Q L/min	T_1 °c	T_2 °c	T_3 °c	T_4 °c
1:00	2.5	29.1	31.1	30.6	45.1
2:00	3.5	29.3	31.1	31.1	44.8
3:00	6.5	27.5	29.9	29.5	40.9
4:00	7	27.1	29.9	29.9	42.5

The best results were taken during the experiments, which are usually from 1PM to 3PM this is the best time to receive solar radiation.

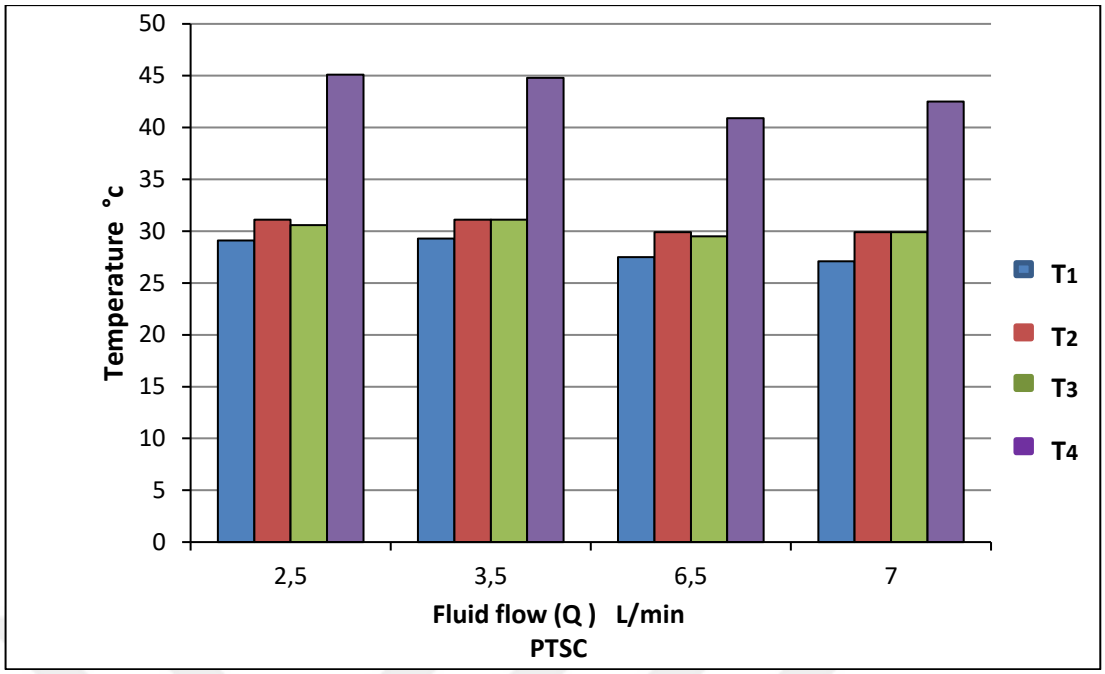

Figure 4.4: Temperatures T1,T2,T3 and T4 with difference flow rates(PTSC).

The results obtained in the second experiment (PTSC with SR) were as in the table (4.4) and Figure (4.5) below.

Table 4.4: Temperature for each point with difference Q (PTSC-SR).

Table PTSC- SR					
Time/h	Q L/min	T_1 °c	T_2 °c	T3 °c	T_4 °c
1:00	2.5	31.5	34.1	33.5	43.5
2:00	3.5	32	32.2	32.4	42.1
3:00	6.5	29.1	31.2	31.9	37.1
4:00	7	28.6	30	30.2	38

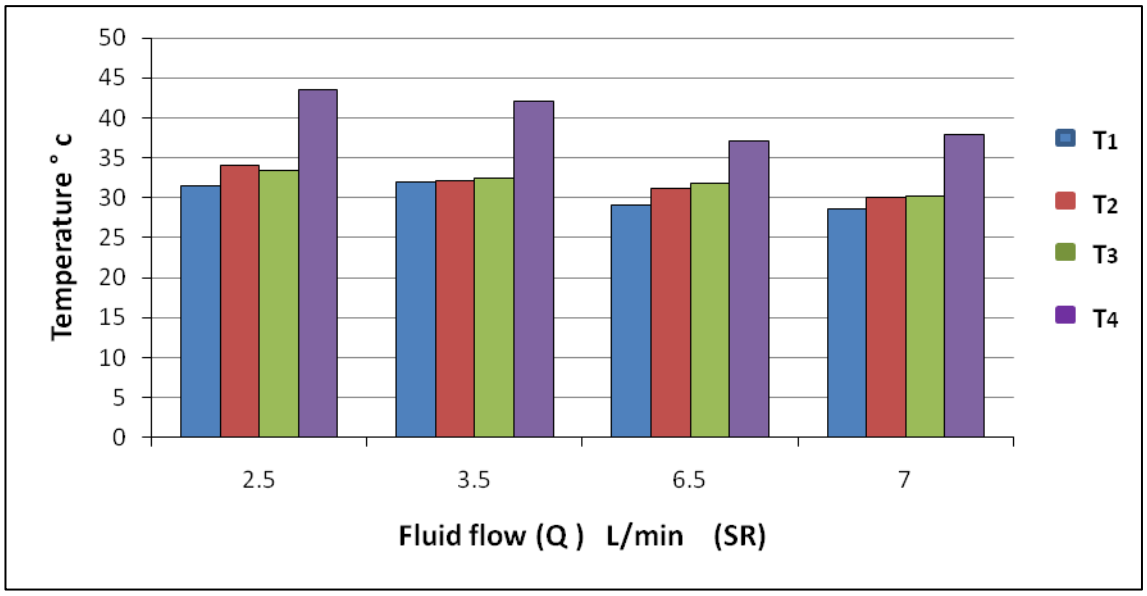

Figure 4.5: Temperatures T_1, T_2, T_3 and T_4 with difference flow rates (PTSC-SR).

4.6 Temperature Distribution on the Absorber Tube Wall

The solar average temperature distribution on the absorber tube outer surface before and after enhancement explicated in (Figures 4.4 and 4.5) respectively as described above. Figure 4.6 (a), (b), (c) and (d) clearly shows the average temperatures distribution (T_1, T_2, T_3 and T_4) on the diameter circumference of tube. It can be observed that the temperature distribution in the conventional PTSC is extremely non-uniform, which has a peak temperature of T_1=30.2, T_2=33.1, T_3=33, T_4= 47.1°C at 2:00 PM. These were the best data with the 3.5 L/min flow rate. The concentration of rays is mainly distributed on the bottom surface of the absorption tube. By contrast, the concentrated average temperature on the entire absorber outer surface after improvement, the value of the average temperature is almost within the range of T_1=32.3, T_2=32.2, T_3=32.1, T_4=43.4 at 2:00PM. These were the best data with the 3.5 L/min flow rate too. Therefore, it can be concluded that the absorber tube can almost be heated Semi-uniformly in the new (PTSC – SR). Tables (4.5) and (4.6) The table shows the temperatures obtained at the flow rate 3.5L /min

Table 4.5: Temperatures obtained at the flow rate 3.5L/ min. (PTSC).

Time	T_1	T_2	T_3	T_4
1:00	29	32	31.8	45.3
2:00	30.2	33.1	33	47.1
3:00	30	32.5	32.5	45.8
4:00	28.1	30.6	30.7	41.3

Table 4.6: Temperatures obtained at the flow rate 3.5L/ min (PTSC-SR)

Time	T_1	T_2	T_3	T_4
1:00	30.2	31	31.1	42
2:00	32.3	32.2	32.1	43.4
3:00	31.7	30.2	30	41.5
4:00	29.5	29	28.8	38

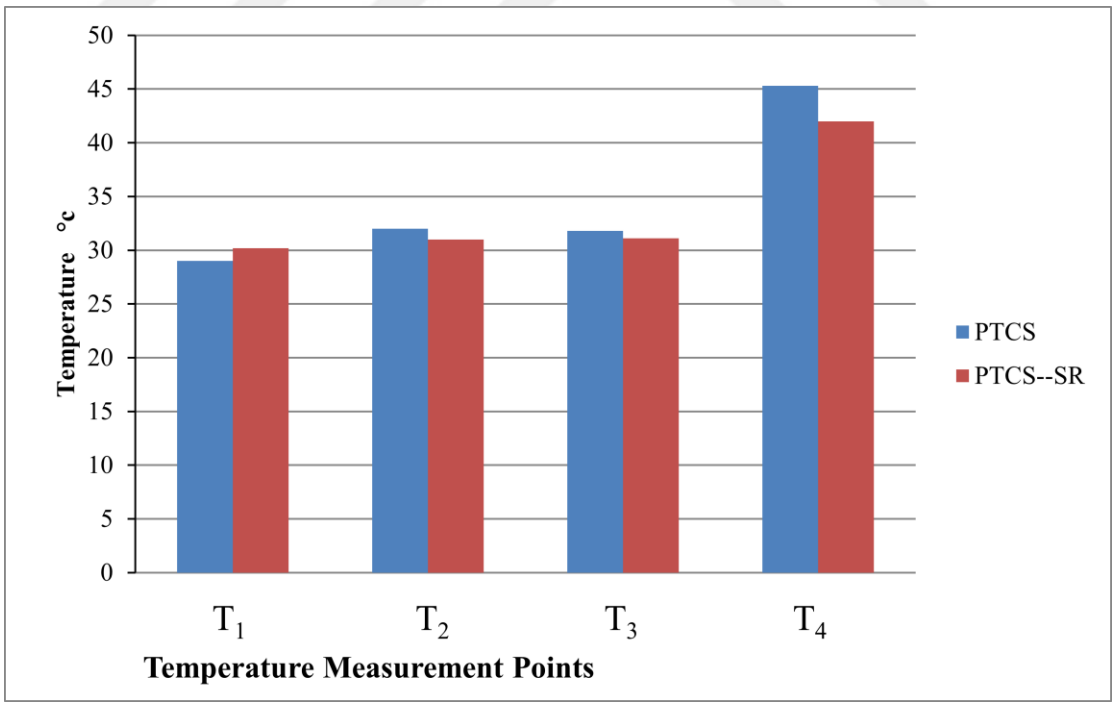

Figure 4.6: (A) show the temperature differences between (PTSC) and (PTSC-SR) At flow rate3.5L. At 1:00PM.

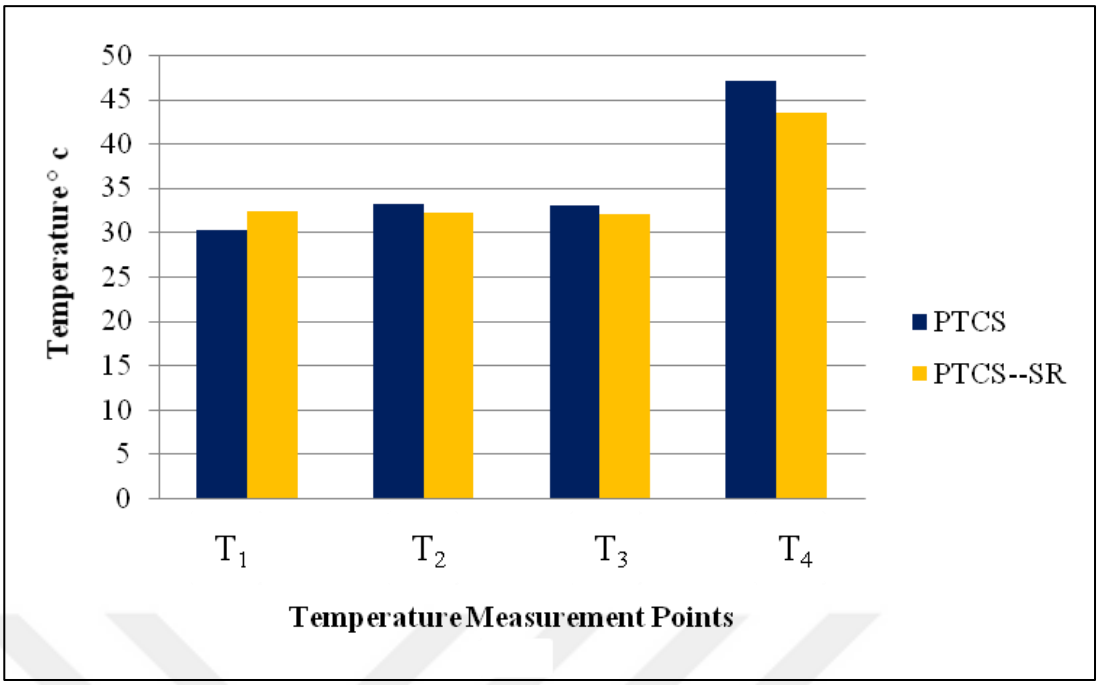

Figure 4.7: (B) show the temperature differences between (PTSC) and (PTSC-SR) At flow rate 3.5L. AT 2:00PM.

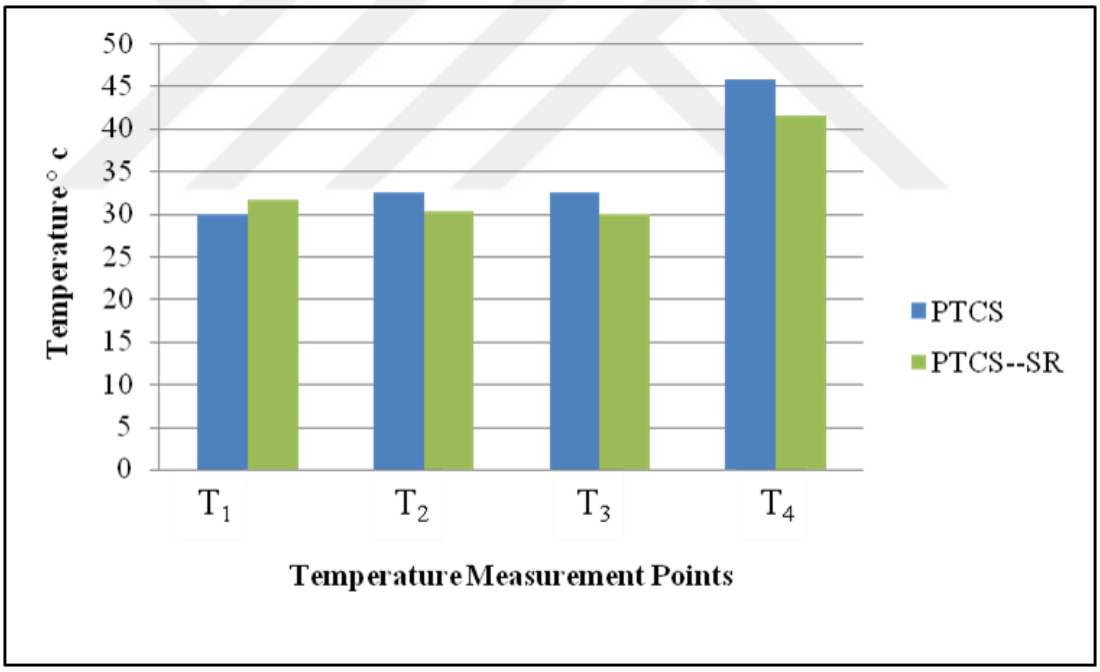

Figure 4.8: (C) show the temperature differences between (PTSC) and (PTSC-SR) At flow rate 3.5L. At 3:00PM.

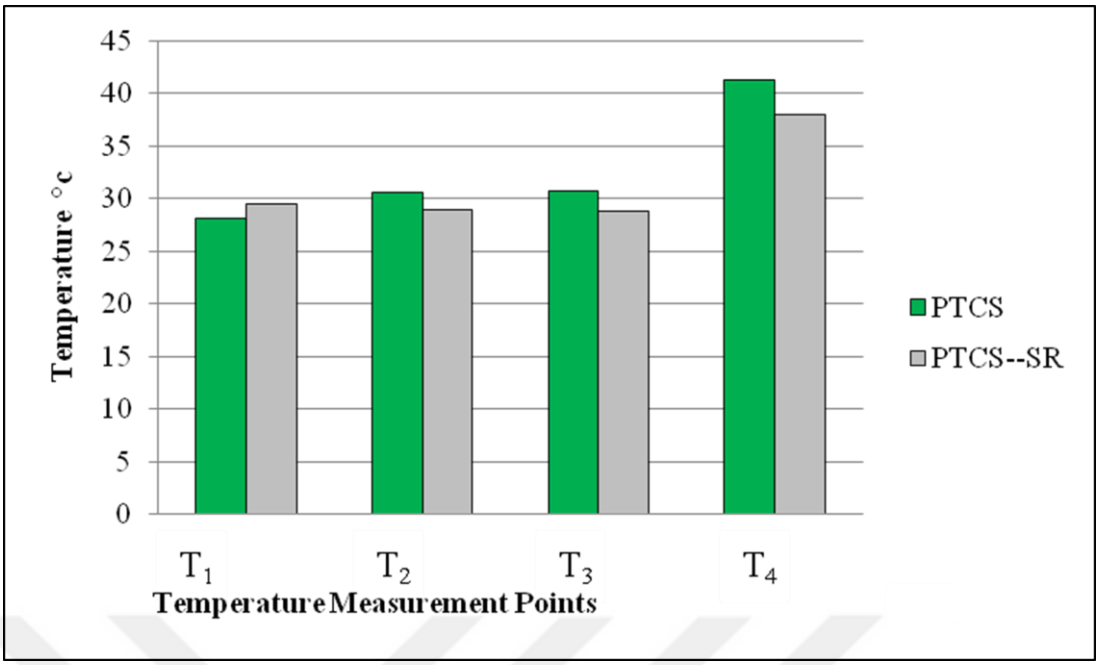

Figure 4.9: (D) show the temperature differences between (PTSC) and (PTSC-SR) At flow rate 3.5L. At 4:00P.

4.7 Useful Heat Gain

The useful heat from the measured input and output temperature was determined from PTSC and PTSC - SR. The flow rate was chosen as 3.5L because it gave the best results in this study. To determine the heat gained, we use the following equation:

$$Q_{gained} = \dot{m} C_p (T_{out} - T_{in}) \quad (4.1)$$

Figure (4.7) shows the difference in heat gain between PTSC and PTSC -SR. At 1:00 PM it was the best time to gain heat, where it was 171W, at 2:00 PM the best time to gain heat. For PTSC -SR device was 244W. Before and after this time, the rate of solar radiation is less, so that the thermal gain is less.

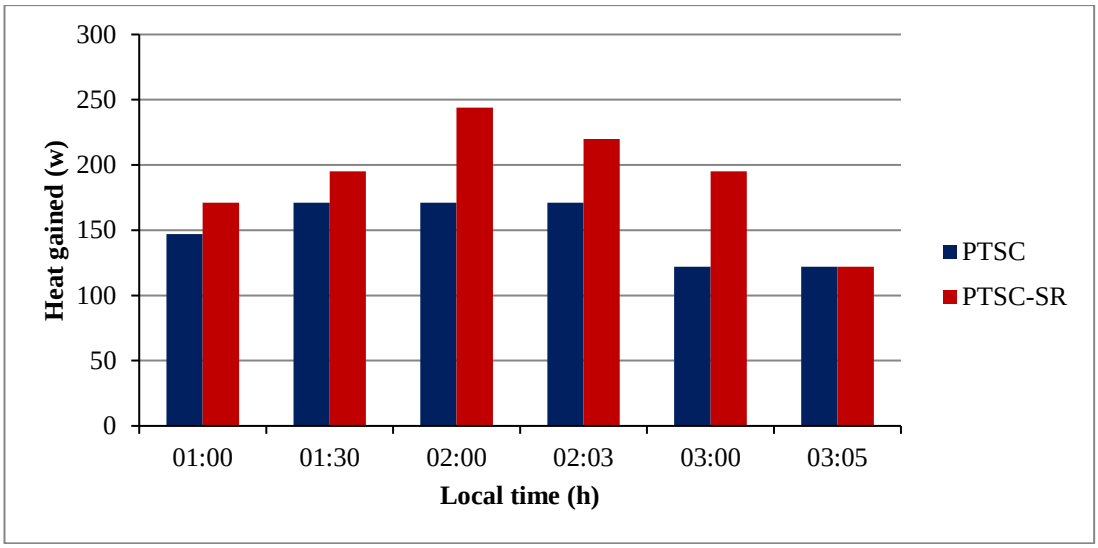

Figure 4.10: Difference in heat gain between PTSC and PTSC –SR.

4.8 Thermal Efficiency

The thermal efficiency of PTSC and PTSC-SR was calculated the heat gain, solar intensity, and aperture area into the following equation.

$$\eta_{th} = \frac{Q_{gained}}{I_{irradiance}\, A_a} \tag{4.2}$$

Figure 4.8 shows the thermal efficiency in the experiment period. It was observed that the efficiency was unstable and fluctuating throughout the test period. The best result of these experiments was (31%) for the PTSC (45%) for the PTSC-SR.

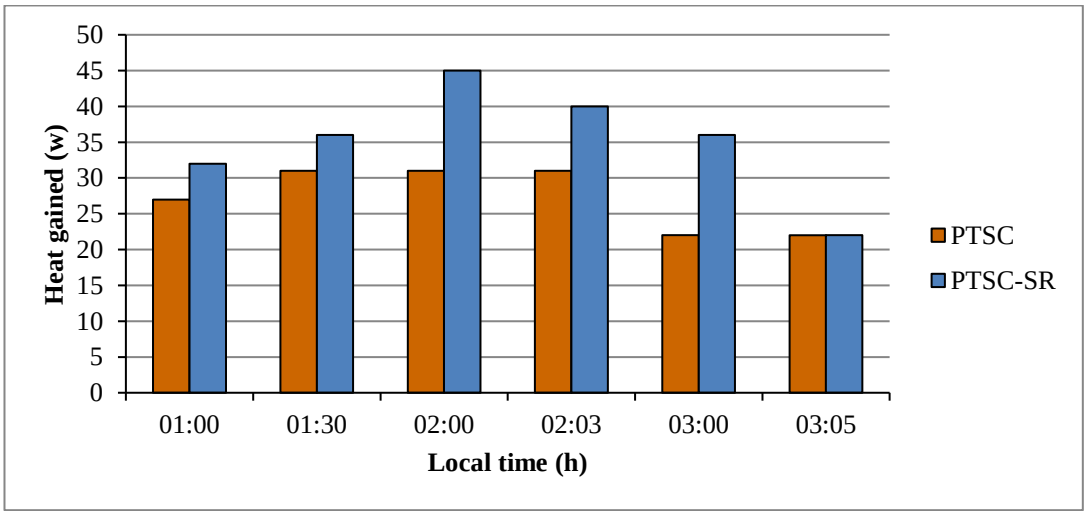

Figure 4.11: Difference in thermal efficiency between PTSC and PTSC –SR.

CHAPTER FIVE

CONCLUSION AND RECOMMENDATIONS

5.1 Conclusion

An experimental model was developed to analyze the performance of PTSC - SR and comparison it with PTSC. The model takes in consideration equations, state of heat transfer and heat transfer mechanism including convection heat transfer inside the absorber and from the absorber to the ambient. The PTSC model was implemented, and the PTSC was applied in addition to the PTSC-SR model, it has the ability to estimate the amount of heat collected by the used fluid, thermal efficiency, heat gain, and outlet temperature of the system. Also, an experimental tests has been conducted at Turkish Aeronautical Association University- Ankara on August 2018, so as to experimentally determine the thermal performance for PTSC and PTSC-SR. Measured results show that, a maximum efficiency of (31%) for PTSC, (45%) for PTSC-SR was obtained, and some factors led to this low resultes such as tubes misalignment, low absorptive of the absorber, poor tracking and geometry errors, small size.

5.2 Recommendations

These recommendations are important for future studies

1. Considering heat loss from connectors.
2. Insulating the pipes will be good in order to prevent heat leakage while the fluid passes through by Insulator.
3. Dependence on an electrical tracker by computer.
4. Increase the size of the parabolic trough solar collector to get better results.
5. Studying the possibility of fixing the reflector so well that it cannot move because of the air conditions.
6. Measure the circumference of the temperature of the perimeter of the tube more accurately.

REFERENCES

[1] A. Florini, “The international energy agency in global energy governance,” Glob. Policy, vol. 2, no. SUPPL.1, pp. 40–50, 2012.

[2] A. E. Outlook and others, “Energy information administration,” Dep. Energy, vol. 92010, no. 9, pp. 1–15, 2010.

[3] M. der Hoeven, “World energy outlook 2012,” Int. Energy Agency Tokyo, Japan, 2013.

[4] A. Fernández-Garc\’\ia, E. Zarza, L. Valenzuela, and M. Pérez, “Parabolic-trough solar collectors and their applications,” Renew. Sustain. Energy Rev., vol. 14, no. 7, pp. 1695–1721, 2010.

[5] W. Spirkl, H. Ries, J. Muschaweck, and A. Timinger, “Optimized compact secondary reflectors for parabolic troughs with tubular absorbers,” Sol. Energy, vol. 61, no. 3, pp. 153–158, 1997.

[6] J. T. Pytilinski, “Solar energy installations for pumping irrigation water,” Sol. Energy, vol. 21, no. 4, pp. 255–262, 1978.

[7] W. W. Shaner and W. S. Duff, “Solar thermal electric power systems: comparison of line-focus collectors,” Sol. Energy, vol. 22, no. 1, pp. 49–61, 1979.

[8] H. Price et al., “Advances in parabolic trough solar power technology,” J. Sol. energy Eng., vol. 124, no. 2, pp. 109–125, 2002.

[9] J. Vázquez and N. Castañeda, “Senertrough. The Collector for Extresol-1. 600 Meters Loop Test in Andasol-1 and Test Unit Description,” in SolarPACES 2008, 14th int symp on conc sol power and chem energy technol, 2008.

[10] G. BARAKOS, “Design, simulation and performance of reflecting parabolic solar collector,” Socrates Program. A Eur. Summer Sch. an Intensive Course ICT Tools PV Systems Eng. Teach. Learn., 2006.

[11] F. A. A. Mutlak, “Design and fabrication of parabolic trough solar collector for thermal energy applications,” Univ. Baghdad, 2011.

[12] A. Sözen, E. Arcaklio\uglu, M. Özalp, and E. G. Kanit, “Solar-energy potential in Turkey,” Appl. Energy, vol. 80, no. 4, pp. 367–381, 2005.

[13] Z. Sen, Solar energy fundamentals and modeling techniques: atmosphere, environment, climate change and renewable energy. Springer Science & Business Media, 2008.

[14] N. Georgescu-Roegen, “Energy and economic myths,” South. Econ. J., pp. 347–381, 1975.

[15] J. E. Braun and J. C. Mitchell, “Solar geometry for fixed and tracking surfaces,” Sol. Energy, vol. 31, no. 5, pp. 439–444, 1983.

[16] B. El Hefni and D. Bouskela, “Solar Collector Modeling,” in Modeling and Simulation of Thermal Power Plants with ThermoSysPro, Springer, 2019, pp. 461–475.

[17] O. Omer, “Badran Design and Implementation of Electro-Mechanical Sun Tracking Parabolic Trough,” Desalination.-220, p. 669, 2008.

[18] T. Markvart and K. Bogus, Solar electricity, vol. 6. John Wiley & Sons, 2000.

[19] H. Mousazadeh, A. Keyhani, A. Javadi, H. Mobli, K. Abrinia, and A. Sharifi, “A review of principle and sun-tracking methods for maximizing solar systems output,” Renew. Sustain. energy Rev., vol. 13, no. 8, pp. 1800–1818, 2009.

[20] M. Donatelli, L. Carlini, and G. Bellocchi, “A software component for estimating solar radiation,” Environ. Model. Softw., vol. 21, no. 3, pp. 411–416, 2006.

[21] H. C. Hottel, “A simple model for estimating the transmittance of direct solar radiation through clear atmospheres,” Sol. energy, vol. 18, no. 2, pp. 129–134, 1976.

[22] S. Alam, S. C. Kaushik, and S. N. Garg, “Computation of beam solar radiation at normal incidence using artificial neural network,” Renew. Energy, vol. 31, no. 10, pp. 1483–1491, 2006.

[23] B. Safari, “A review of energy in Rwanda,” Renew. Sustain. Energy Rev., vol. 14, no. 1, pp. 524–529, 2010.

[24] H. G. Riveros and A. I. Oliva, “Graphical analysis of sun concentrating collectors,” Sol. energy, vol. 36, no. 4, pp. 313–322, 1986.

[25] S. M. Jeter, “Optical and thermal effects in linear solar concentrating collectors,” 1979.

[26] V. E. Dudley et al., “Test results: SEGS LS-2 solar collector, Sandia National Labs,” Albuquerque, NM (United States), p. 1994, 1994.

[27] F. Lippke, “Simulation of the part-load behavior of a 30MWe SEGS plant. Albuquerque.” New Mexico: Solar Thermal Technology Department and Sandia National, 1995.

[28] E. Jacobson, N. Ketjoy, S. Nathakaranakule, and W. Rakwichian, “Solar parabolic trough simulation and application for a hybrid power plant in Thailand,” Sci. Asia, vol. 32, no. 2, pp. 187–199, 2006.

[29] O. Garc\’\ia-Valladares and N. Velázquez, “Numerical simulation of parabolic trough solar collector: Improvement using counter flow concentric circular heat exchangers,” Int. J. Heat Mass Transf., vol. 52, no. 3–4, pp. 597–609, 2009.

[30] S. Thepa, K. Kirtikara, J. Hirunlabh, and J. Khedari, “Improving indoor conditions of a Thai-style mushroom house by means of an evaporative cooler and continuous ventilation,” Renew. energy, vol. 17, no. 3, pp. 359–369, 1999.

[31] L. Hodges, “Resource Letter SE-2: Solar Energy,” Am. J. Phys., vol. 50, no. 10, pp. 876–881, 1982.

[32] M. Li and L. L. Wang, “Investigation of evacuated tube heated by solar trough concentrating system,” Energy Convers. Manag., vol. 47, no. 20, pp. 3591–3601, 2006.

[33] A. Kahrobaian and H. R. Malekmohammadi, “Exergy optimization applied to linear parabolic,” J. Algorithms Comput., vol. 42, no. 1, pp. 131–144, 2013.

[34] B. Norton, D. E. Prapas, P. C. Eames, and S. D. Probert, “Measured performances of curved inverted-Vee, absorber compound parabolic concentrating solar-energy collectors,” Sol. energy, vol. 43, no. 5, pp. 267–279, 1989.

[35] S. Kalogirou, “Parabolic trough collector system for low temperature steam generation: design and performance characteristics,” Appl. Energy, vol. 55, no. 1, pp. 1–19, 1996.

[36] S. Kalogirou, “Use of parabolic trough solar energy collectors for sea-water desalination,” Appl. Energy, vol. 60, no. 2, pp. 65–88, 1998.

[37] M. Mazloumi, M. Naghashzadegan, and K. Javaherdeh, “Simulation of solar lithium bromide--water absorption cooling system with parabolic trough collector,” Energy Convers. Manag., vol. 49, no. 10, pp. 2820–2832, 2008.

[38] Y. Aldali, T. Muneer, and D. Henderson, “Solar absorber tube analysis: thermal simulation using CFD,” Int. J. Low-Carbon Technol., vol. 8, no. 1, pp. 14–19, 2011.

[39] “forecast-5days @ www.mgm.gov.tr.” .

[40] Z. D. Cheng, Y. L. He, and F. Q. Cui, “Numerical study of heat transfer enhancement by unilateral longitudinal vortex generators inside parabolic trough solar receivers,” Int. J. Heat Mass Transf., vol. 55, no. 21–22, pp. 5631–5641, 2012.

[41] P. Wang, D. Y. Liu, and C. Xu, “Numerical study of heat transfer enhancement in the receiver tube of direct steam generation with parabolic trough by inserting metal foams,” Appl. Energy, vol. 102, pp. 449–460, 2013.

[42] R. Almanza, A. Lentz, and G. Jimenez, “Receiver behavior in direct steam generation with parabolic troughs,” Sol. Energy, vol. 61, no. 4, pp. 275–278, 1997.

[43] V. Flores and R. Almanza, “Behavior of the compound wall copper--steel receiver with stratified two-phase flow regimen in transient states when solar irradiance is arriving on one side of receiver,” Sol. Energy, vol. 76, no. 1–3, pp. 195–198, 2004.

[44] G. Delussu, “A qualitative thermo-fluid-dynamic analysis of a CO2 solar pipe receiver,” Sol. energy, vol. 86, no. 3, pp. 926–934, 2012.

[45] K. Wang, Y. He, and Z. Cheng, “A design method and numerical study for a new type parabolic trough solar collector with uniform solar flux distribution,” Sci. China Technol. Sci., vol. 57, no. 3, pp. 531–540, 2014.

[46] Y. Qiu, M.-J. Li, Y.-L. He, and W.-Q. Tao, “Thermal performance analysis of a parabolic trough solar collector using supercritical CO2 as heat transfer fluid under non-uniform solar flux,” Appl. Therm. Eng., vol. 115, pp. 1255–1265, 2017.